

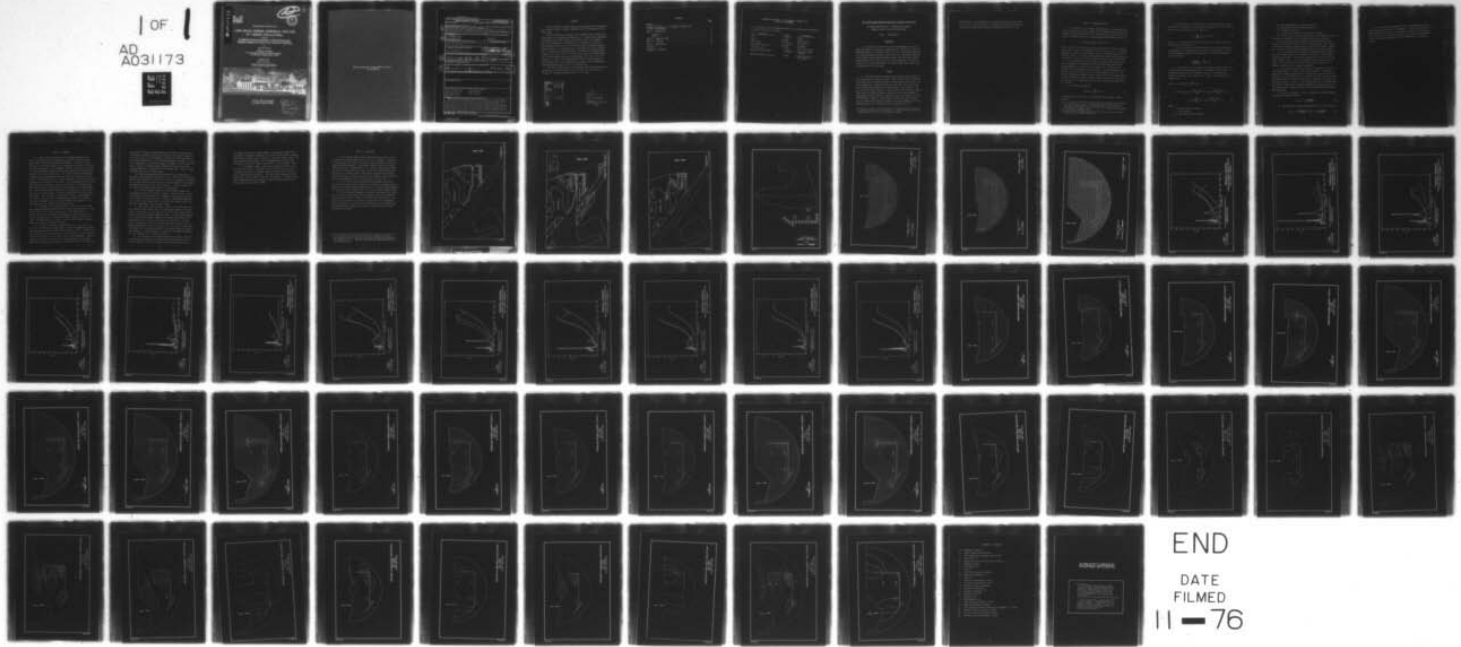
AD-A031 173 ARMY ENGINEER WATERWAYS EXPERIMENT STATION VICKSBURG MISS F/G 8/3  
LONG BEACH HARBOR NUMERICAL ANALYSIS OF HARBOR OSCILLATIONS. RE--ETC(U)  
SEP 76 J R HOUSTON

UNCLASSIFIED

WES-MP-H-76-20-3

NL

| OF |  
AD  
A031173



END

DATE  
FILMED

11 - 76

AD A031173



D  
FB.



MISCELLANEOUS PAPER H-76-20

## LONG BEACH HARBOR NUMERICAL ANALYSIS OF HARBOR OSCILLATIONS

Report 3

ALTERNATE PLANS FOR PIER J COMPLETION AND  
TANKER TERMINAL PROJECT (62-AND 82-FT DEPTHS)

by

James R. Houston

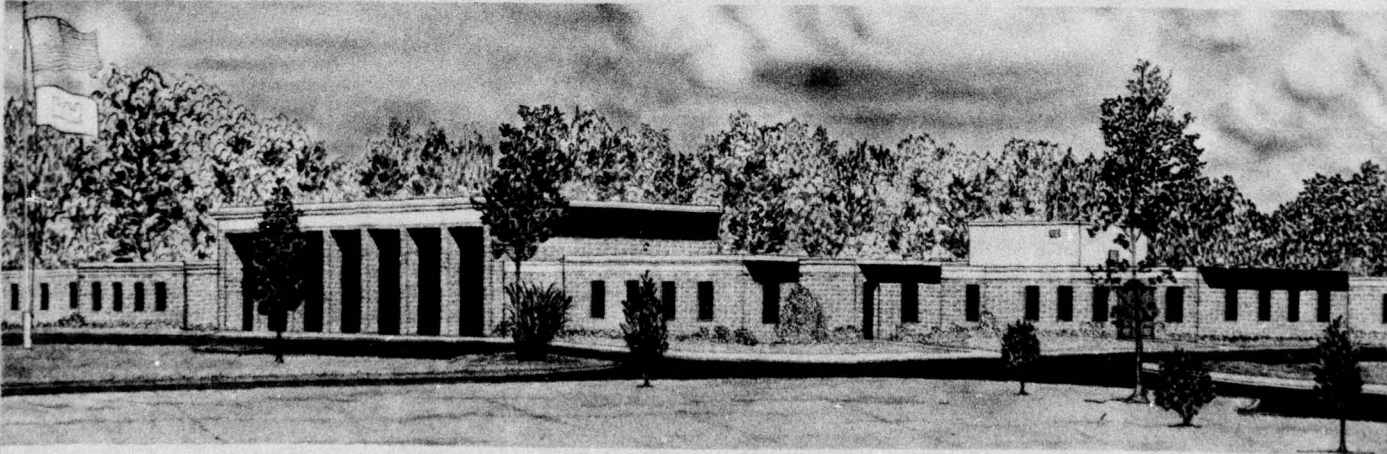
Hydraulics Laboratory

U. S. Army Engineer Waterways Experiment Station  
P. O. Box 631, Vicksburg, Miss. 39180

September 1976

Report 3 of a Series

Approved For Public Release; Distribution Unlimited



Prepared for Port of Long Beach  
Long Beach, California 90801

D D C  
RECEIVED  
OCT 27 1976  
RECORDED  
D

**Destroy this report when no longer needed. Do not return  
it to the originator.**

Unclassified

SECURITY CLASSIFICATION OF THIS PAGE (When Data Entered)

REPORT DOCUMENTATION PAGE		READ INSTRUCTIONS BEFORE COMPLETING FORM
1. REPORT NUMBER Miscellaneous Paper H-76-20	2. GOVT ACCESSION NO.	3. RECIPIENT'S CATALOG NUMBER
4. TITLE (and Subtitle) LONG BEACH HARBOR NUMERICAL ANALYSIS OF HARBOR OSCILLATIONS: Report 3, ALTERNATE PLANS FOR PIER J COMPLETION AND TANKER TERMINAL PROJECT (62- AND 82-FT DEPTHS).		5. TYPE OF REPORT & PERIOD COVERED Report 3 of a series
7. AUTHOR(s) James R. Houston		6. PERFORMING ORG. REPORT NUMBER WES-76-4
9. PERFORMING ORGANIZATION NAME AND ADDRESS U. S. Army Engineer Waterways Experiment Station Hydraulics Laboratory P. O. Box 631, Vicksburg, Mississippi 39180		10. PROGRAM ELEMENT, PROJECT, TASK AREA & WORK UNIT NUMBERS
11. CONTROLLING OFFICE NAME AND ADDRESS Port of Long Beach Long Beach, California 90801		12. REPORT DATE September 1976
14. MONITORING AGENCY NAME & ADDRESS (if different from Controlling Office) WES-MP-H-76-20-3		13. NUMBER OF PAGES 61
15. SECURITY CLASS. (of this report) Unclassified		
15a. DECLASSIFICATION/DOWNGRADING SCHEDULE 63p		
16. DISTRIBUTION STATEMENT (of this Report) Approved for public release, distribution unlimited.		
17. DISTRIBUTION STATEMENT (or the abstract entered in Block 20, if different from Report) Miscellaneous paper Sep 75 - Mar 76		
18. SUPPLEMENTARY NOTES		
19. KEY WORDS (Continue on reverse side if necessary and identify by block number) Finite element method      Numerical analysis Harbor oscillations      Piers (Docks) Long Beach Harbor      Tanker terminals Mathematical models		
20. ABSTRACT (Continue on reverse side if necessary and identify by block number) A hybrid finite element numerical model was used to calculate harbor response for three alternate geometrical plans and two water depths for the Pier J completion and tanker terminal project of Long Beach Harbor. The numerical model calculates harbor oscillation for harbors of arbitrary shape and variable depth. Three finite element grids which covered areas only in the immediate vicinity of the breakwater-protected tanker terminal area were used to calculate the response of this area to incident waves with periods from 30 sec to approximately 6 min.		

DD FORM 1 JAN 73 1473 EDITION OF 1 NOV 65 IS OBSOLETE

Unclassified

SECURITY CLASSIFICATION OF THIS PAGE (When Data Entered)

038100

JB

PREFACE

The investigation reported herein was authorized by the Long Beach Port Authority under a contract, Agreement No. WES 76-4, dated 12 September 1975.

The investigation was conducted from September 1975 to March 1976 by personnel of the Hydraulics Laboratory, U. S. Army Engineer Waterways Experiment Station (WES), under the direction of Mr. H. B. Simmons, Chief of the Hydraulics Laboratory, Dr. R. W. Whalin, Chief of the Wave Dynamics Division, Mr. D. D. Davidson, Chief of the Wave Research Branch, and Mr. C. E. Chatham, Chief of the Harbor Wave Action Branch. Mr. J. R. Houston, Research Physicist, conducted the investigation and prepared this report. Mr. R. R. Bottin, Jr., aided in the development of the finite element grids and the plotting of the data. Drs. H. S. Chen and C. C. Mei of the Massachusetts Institute of Technology provided documentation of the hybrid finite element computer program they developed and materials to aid in its utilization.

Directors of WES during the investigation and the preparation and publication of this report were COL G. H. Hilt, CE, and COL John L. Cannon, CE. Technical Director was Mr. F. R. Brown.

ACCESSION for	
NTIS	White Section <input checked="" type="checkbox"/>
DDC	Buff Section <input type="checkbox"/>
UNANNOUNCED	<input type="checkbox"/>
JUSTIFICATION.....	
BY.....	
DISTRIBUTION/AVAILABILITY CODES	
DISL	AVAIL. AND/OR SPECIAL
A	

D D C  
REF ID: A  
OCT 27 1976  
R E C U L T I C  
D

CONTENTS

	<u>Page</u>
PREFACE . . . . .	1
CONVERSION FACTORS, U. S. CUSTOMARY TO METRIC (SI)	
UNITS OF MEASUREMENT . . . . .	3
PART I: INTRODUCTION . . . . .	4
Objective . . . . .	4
Scope . . . . .	4
PART II: NUMERICAL MODEL . . . . .	6
PART III: RESULTS . . . . .	10
PART IV: CONCLUSIONS . . . . .	13
PLATES 1-47	
APPENDIX A: NOTATION	

CONVERSION FACTORS, U. S. CUSTOMARY TO METRIC (SI)  
UNITS OF MEASUREMENT

U. S. customary units of measurement used in this report can be converted to metric (SI) units as follows:

Multiply	By	To Obtain
feet	0.3048	metres
acres	4046.856	square metres
cubic yards	0.7645549	cubic metres
tons (2000 lb, mass)	907.1847	kilograms
feet per second	0.3048	metres per second
square feet per second	0.09290304	square metres per second
feet per second per second	0.3048	metres per second per second

LONG BEACH HARBOR NUMERICAL ANALYSIS OF HARBOR OSCILLATIONS

ALTERNATE PLANS FOR PIER J COMPLETION AND TANKER  
TERMINAL PROJECT (62- AND 82-FT DEPTHS)

PART I: INTRODUCTION

Objective

1. The objective of this study was to investigate by use of a numerical model the response to long-period wave excitation of six proposed alternatives for modifications to Pier J in Long Beach Harbor for oil tanker berthing and general cargo facilities. Wave-height amplification factors and normalized maximum current velocities were plotted versus wave period at the proposed oil tanker terminals to ascertain whether or not significant harbor oscillations might occur which would pose problems to ship berthing.

Scope

2. The tanker terminal configurations (plans) were considered in the study; plan 1 is shown in Plate 1. Both 300- and 600-ft\* openings at the east end of the basin and 62- and 82-ft depths were tested. The basin geometry was slightly different for the 82-ft depth since there was a cutback with dimensions of approximately 160 by 1550 ft at the east end of the basin (Plate 2). Plan 2 (Plate 3) was similar to plan 1 except that the proposed landfill addition to Pier J was reduced to approximately 50 acres with an open-water area to the east for mooring two 250,000-dwt tankers. Water depths of 62 and 82 ft were tested. Waves incident from a direction normal to the main breakwater face with periods from 30 sec to 300-340 sec were considered for both

---

\* A table of factors for converting U. S. customary units of measurement to metric (SI) units is presented on page 3.

configurations. Wave amplitude and current velocities were calculated every 5 sec for the period range. Resonant peaks also were defined by considering incident wave periods in increments as low as 0.25 sec.

## PART II: NUMERICAL MODEL

3. The response of the tanker terminal basin to long wave excitation was determined by using a hybrid finite element numerical model developed recently by Chen and Mei\* at the Massachusetts Institute of Technology. The model solves the following generalized Helmholtz equation:

$$\nabla \cdot [h(x,y)\nabla\phi(x,y)] + \frac{w^2}{g} \phi(x,y) = 0 \quad (1)$$

where  $\phi(x,y)**$  is the velocity potential defined by  $u(x,y) = -\nabla\phi(x,y)$ , with  $u(x,y)$  being a two-dimensional velocity vector and  $w$  an angular frequency. Equation 1 governs small amplitude undamped oscillations of water in a basin of arbitrary shape and variable depth forced by periodic long waves. It has been further assumed that the flow is irrotational.

4. The boundary condition along the shoreline and along the detached breakwater surrounding the three proposed berths is that the normal component of the velocity be equal to zero. Therefore, the breakwater is considered as a solid barrier. No special boundary conditions are made to account for the storage tankers in plan 2 or any vessels utilizing the tanker terminal basin, since for long-period waves of small amplitude ship heave equals incident wave height. Therefore, the vessels do not significantly alter the oscillation characteristics of the basin.

5. The Helmholtz equation:

$$\nabla^2\phi(x,y) + \frac{w^2}{gh} \phi(x,y) = 0 \quad (2)$$

is the governing equation for a constant-depth ocean region outside the basin.

---

\* H. S. Chen and C. C. Mei, "Oscillations and Wave Forces in an Off-shore Harbor (Applications of the Hybrid Finite Element Method to Water-Wave Scattering)," Report No. 190, 1974, Massachusetts Institute of Technology, Cambridge, Mass.

\*\* For convenience, symbols and unusual abbreviations are listed and defined in the Notation (Appendix A).

6. For a harbor in a semi-infinite ocean with a straight coast-line there is an incident, reflected, and scattered wave. The scattered wave has a velocity potential  $\phi_s$  given by

$$\phi_s = \sum_{n=0}^{\infty} \alpha_n H_n(kr) \cos n\theta \quad (3)$$

where  $\alpha_n$  are unknown coefficients and  $H_n(kr)$  are Hankel functions of the first kind of order  $n$ .

7.  $\phi_s$  satisfies the radiation condition that the scattered wave must behave as an outgoing wave at infinity. This condition is known as the Sommerfeld radiation condition and may be expressed mathematically as follows:

$$\lim_{r \rightarrow \infty} \sqrt{r} \left( \frac{\partial}{\partial r} - ik \right) \phi_s = 0 \quad (4)$$

8. Chen and Mei used a calculus of variations approach and obtained a Euler-Lagrange formulation of the boundary value problem. The following functional with the property that it is stationary with respect to arbitrary first variations of  $\phi(x,y)$  was constructed by Chen and Mei:

$$\begin{aligned} F(\phi) &= \iint \frac{1}{2} \{ h(\nabla \phi)^2 - \frac{w^2}{g} \phi^2 \} dA \\ &+ \frac{1}{2} \oint \{ h(\phi_R - \phi_I) \frac{\partial(\phi_R - \phi_I)}{\partial n_a} da - \oint h \phi_a \frac{\partial(\phi_R - \phi_I)}{\partial n_a} da \\ &- \oint h \phi_a \frac{\partial \phi_I}{\partial n_a} da + \oint h \phi_I \frac{\partial(\phi_R - \phi_I)}{\partial n_a} da \end{aligned} \quad (5)$$

where

$A$  = region inside the harbor

$\oint$  = line integral

$\phi_R$  = far field velocity potential

$\phi_I$  = velocity potential of the incident wave

$n_a$  = unit normal vector outward from region A

a = boundary of region A

$\phi_a$  = total velocity potential evaluated on boundary a

9. Proof was given by Chen and Mei that the stationarity of this functional is equivalent to the original boundary value problem.

10. The integral equation obtained from extremizing the functional is solved by utilizing the finite element method. This method is a technique of numerical approximation that involves dividing a domain into a number of nonoverlapping subdomains which are called elements.

11. The solution of the problem is approximated within each element by suitable interpolation functions in terms of a finite number of unknown parameters. These unknown parameters are the values of the field variable  $\phi(x,y)$  at a finite number of points which are called nodes. The relations for individual elements are combined into a system of equations for all unknown parameters.

12. In the region outside the basin, the velocity potentials are solved analytically in terms of unknown coefficients. The region is considered a single element with an "interpolation function" given by Equation 3. The infinite series is terminated at some finite value such that the addition of further terms does not significantly influence the calculated values of  $\phi(x,y)$ . The resulting equation is combined with the system of equations for unknown parameters at nodal points within the basin and this complete system is solved using Gaussian elimination matrix methods.

13.  $\eta(x,y)$  is related to  $\phi(x,y)$  through the linearized dynamic free surface boundary condition

$$\eta(x,y) = -\frac{1}{g} \frac{\partial \phi(x,y)}{\partial t} \quad (6)$$

14. The horizontal velocity components have the following form:

$$u(x,y) = -\frac{g}{w} \frac{\partial \eta(x,y)}{\partial x}; \quad v(x,y) = -\frac{g}{w} \frac{\partial \eta(x,y)}{\partial y} \quad (7)$$

15. The hybrid finite element method (so named by Chen and Mei because the method involves the combination of analytical and finite element numerical solutions) is a steady-state solution of the boundary value problem. The response of a harbor to an arbitrary forcing function can be easily determined within the framework of a linearized theory.

### PART III: RESULTS

16. Plate 4 shows the locations of the tanker terminals and Plates 5-7 show the finite element grids for STFP 2 (600) with 62-ft depth, STFP 2 (600) with 82-ft depth, and STFP 3. The grids for STFP (300) with 62- and 82-ft depths are not shown but are similar to the grids for STFP (600) except for the breakwater opening. Plates 8-13 are plots of normalized maximum current velocity versus wave period at each tanker terminal for the six modifications. The current velocity multiplied by the incident wave amplitude in feet gives velocity in units of feet per second. The velocities have no vertical component or variation since only long waves are considered in this study. Also, the maximum velocity over one wave period is plotted. Plates 14-19 are plots of the wave-height amplification factor versus wave period in seconds at each tanker terminal. The wave-height amplification factor is defined at a point inside the basin as the wave height at the point divided by twice the incident wave height. This definition of amplification factor is traditional and is a result of the fact that the standing wave height for a straight coast with no harbor would be twice the incident wave height due to the superposition of the incident and reflected waves.

17. Plan STFP 2 (300) and plan STFP 2 (600) for the 62-ft depth have normalized maximum current velocity (NMCV) resonant peaks of 57 and 280 sec and 57.5 and 260 sec, respectively. The NMCV patterns in Plates 20 and 22 for the peaks of approximately 1 min are very similar for the two plans with the velocities somewhat larger for plan STFP 2 (600). The NMCV patterns in Plates 21 and 23 for the peaks of approximately 4-1/2 min are virtually identical.

18. Plan STFP 3 has NMCV resonant peaks of 55, 55.5, 106, and 350 sec. The NMCV peaks of approximately 1 min are substantially larger than similar peaks for plan STFP 2 (300) and STFP 2 (600). The NMCV patterns in Plates 24 and 25 are similar to the patterns in Plates 20 and 22 with high velocities occurring near corners of the breakwater. Large velocities also occur in the area of the storage tankers. The 106-sec NMCV peak is substantially larger for plan STFP 3 than for the other two

plans; Plate 26 shows the NMCV pattern for this peak. Velocities are very large at terminals 2 and 3 as a result of the antinode forming in the inside corner of the breakwater (see Plate 40 for the contours of wave-height amplification). The 350-sec NMCV peak at terminal 1 is similar in magnitude to the 4-1/2-min peaks at terminal 1 for the other two plans. However, the NMCV peaks at terminals 2 and 3 are less than corresponding peaks of plans STFP (300) and STFP (600). Plate 27 shows the NMCV pattern for the 350-sec peak.

19. Wave-height amplification factors are quite similar for plans STFP (300) and STFP (600) (Plates 14-16). Contours of wave-height amplification presented in Plates 34-37 are also very similar. Antinodes for the 1-min peak are located at the two inside corners of the detached breakwater and along the shore near terminal 3. A single antinode in the center of the basin forms for the 4-1/2-min peak.

20. The 1-min peaks for STFP 3 are substantially larger than corresponding peaks for the other two plans. Antinodes form in the inside corners of the breakwater, near terminal 3, and along the corner of the landfill (Plates 38 and 39). Contours of wave-height amplification for the 350-sec peak of STFP 3 (Plate 41) are similar to the contours for plans STFP 2 (300) and STFP 2 (600).

21. Plans STFP 2 (300) and STFP 2 (600) for the 82-ft depth have NMCV resonant peaks (Plates 28-31) and wave-height amplification peaks (Plates 42-45) similar to the peaks for the 62-ft depth except that the peaks for the 82-ft depth are somewhat larger. This difference appears to be caused by the geometry change of the cutback with dimensions of approximately 160 by 1550 ft at the east end of the basin. For example, a comparison of Plates 34 and 42, which show contours of wave-height amplification for the 1-min peaks for STFP 2 (300), reveals that the cutback has increased the height of the antinode along the landfill near terminal 3. The antinode in the corner of the detached breakwater has also increased for the cutback conditions.

22. The contours of wave-height amplification (Plates 46 and 47) and NMCV patterns (Plates 32 and 33) are almost identical for the 62- and 82-ft depths of STFP 3; the amplification factors and velocities

are larger for the 62-ft depth, however. This difference may result from greater reflection of energy for the 82-ft depth as waves propagate from the 60-ft depths outside the basin to the 82-ft depths inside. The same effect might contribute to the lower amplification factors and velocities for the 82-ft depth of plans STFP 2 (300) and STFP 2 (600).

23. In summary, larger 1- and 2-min resonant oscillations occur for plan STFP 3 than for plans STFP 2 (300) and STFP 2 (600). The 4- to 6-min oscillations are somewhat larger for plans STFP 2 (300) and STFP 2 (600) than for plan STFP 3. The oscillation characteristics of plans STFP 2 (300) and STFP 2 (600) are very similar. Oscillations are also somewhat greater for all plans for the 62-ft depth than for the 82-ft depth with the 160-ft cutback.

#### PART IV: CONCLUSIONS

24. The resonant peaks of the normalized maximum current velocity and the wave-height amplification factor do not appear to preclude safe berthing at the terminal areas given proper mooring practices and adequate mooring equipment. The resonant response peaks for incident waves with periods of approximately 1 to 2 min are significantly larger for the 62-ft depth STFP 3 plan than for the 62-ft depth STFP 2 plans. Whether or not incident waves in this period range excite significant ship motion depends upon ship characteristics (length, width, and draft) and mooring conditions (type of lines, amount of slack, etc.).

25. The incident wave spectrum and ship response versus wave period curves must be known in addition to the harbor response curves of Plates 8-19 to definitively determine whether or not ship surge problems resulting from harbor resonance will occur in the tanker terminal basin.

26. Until detailed information on moored ship response as a function of incident wave amplitude and frequency is obtained, definitive conclusions on the precise amount of ship motion cannot be made. However, the oscillations of the tanker terminal basin are significantly smaller than typical oscillations noted throughout the Los Angeles and Long Beach Harbors complex in the numerical study performed for the entire harbor complex.\*

---

\* J. R. Houston, "Long Beach Harbor Numerical Analysis of Harbor Oscillations; Report 1, Existing Conditions and Proposed Improvements" (in preparation), U. S. Army Engineer Waterways Experiment Station, CE, Vicksburg, Miss.

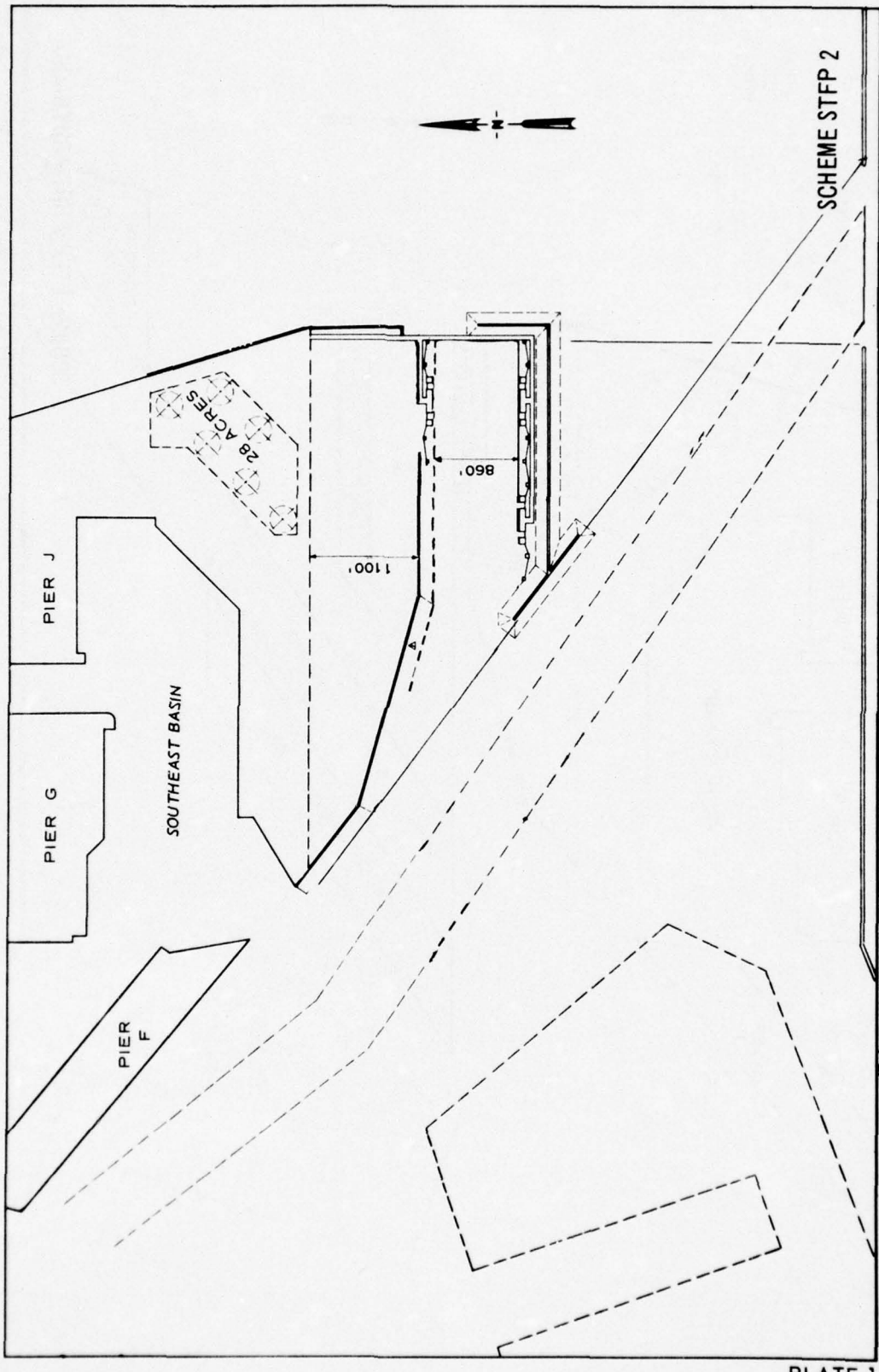
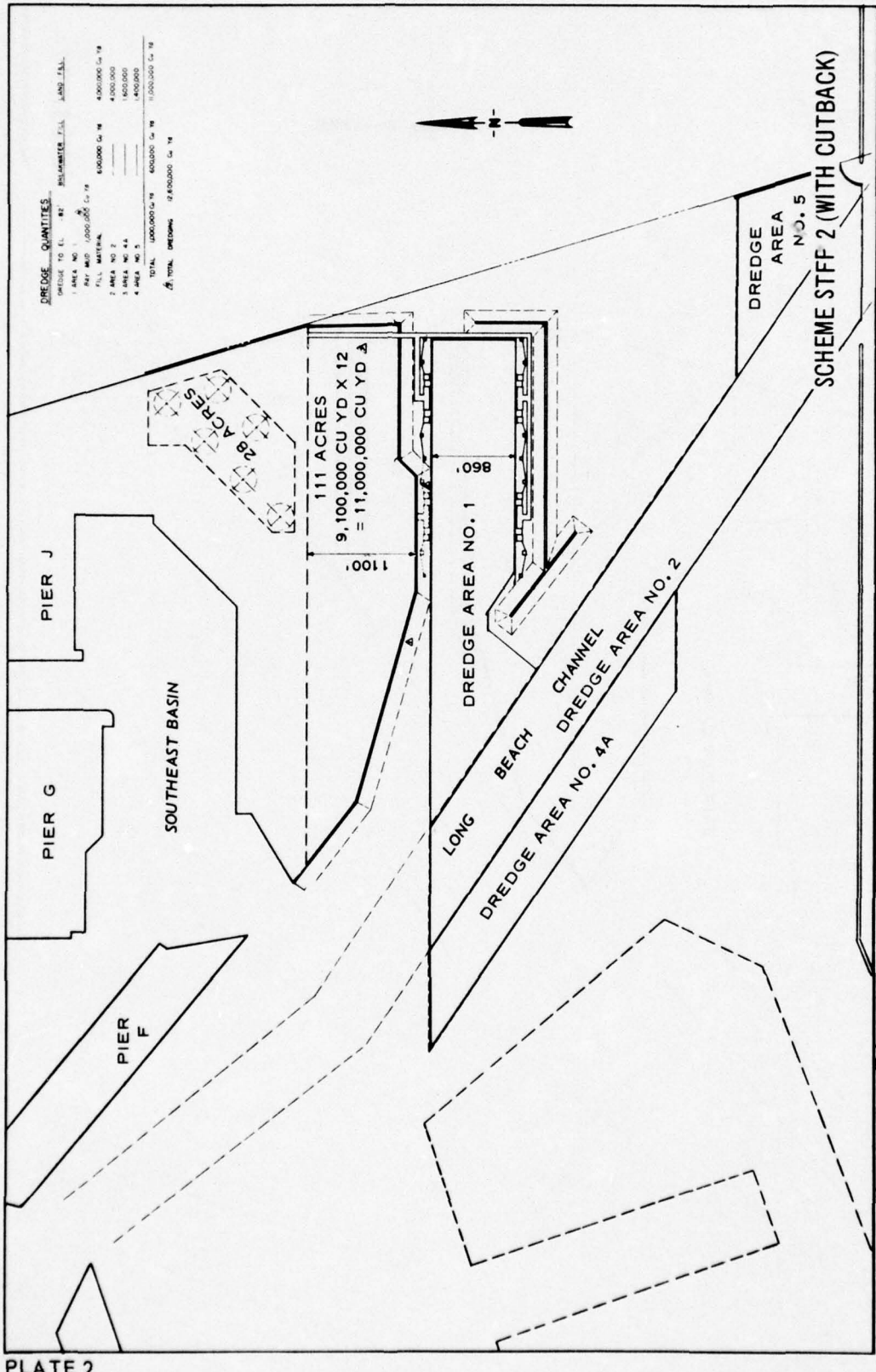


PLATE 1



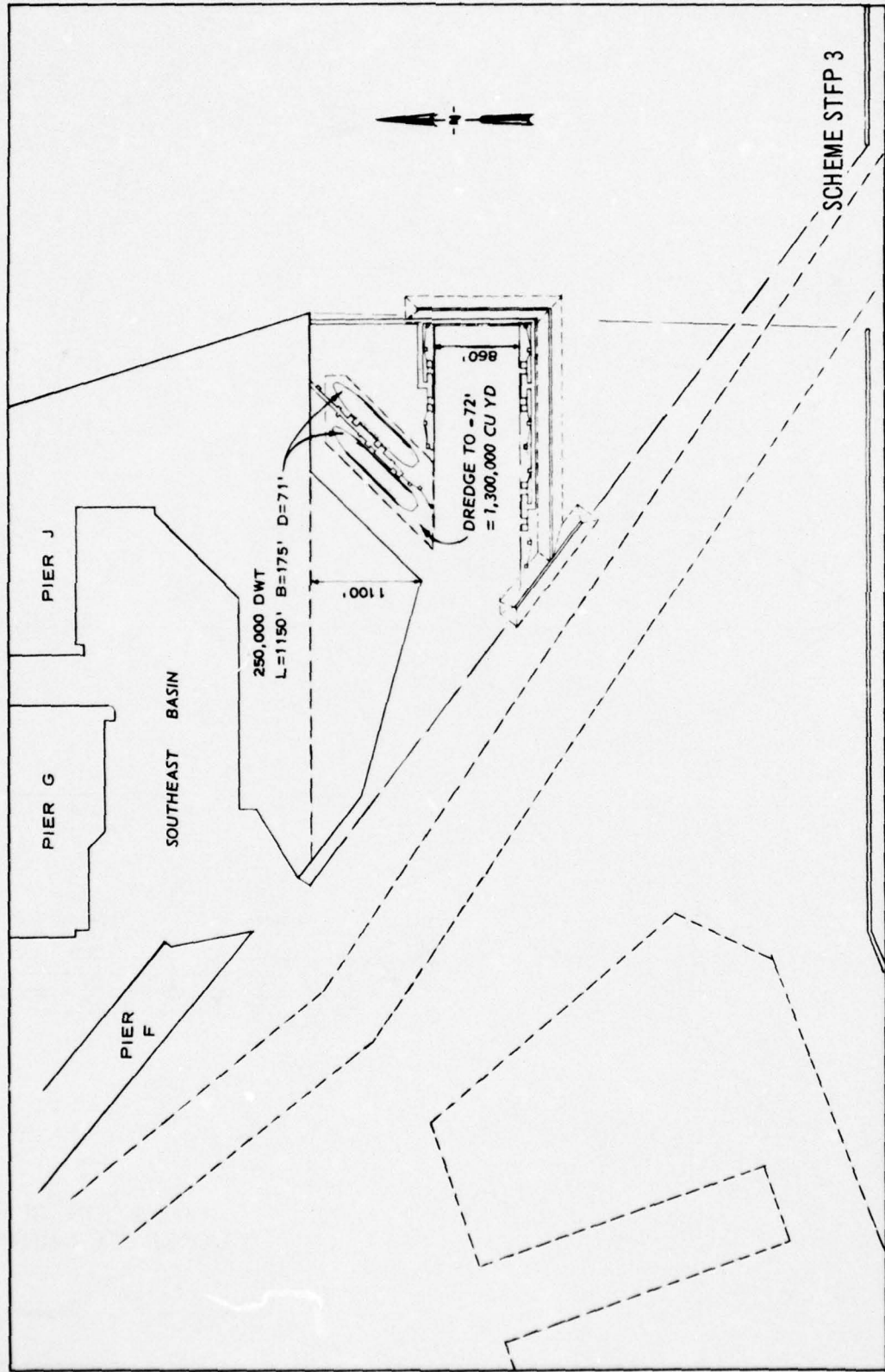


PLATE 3

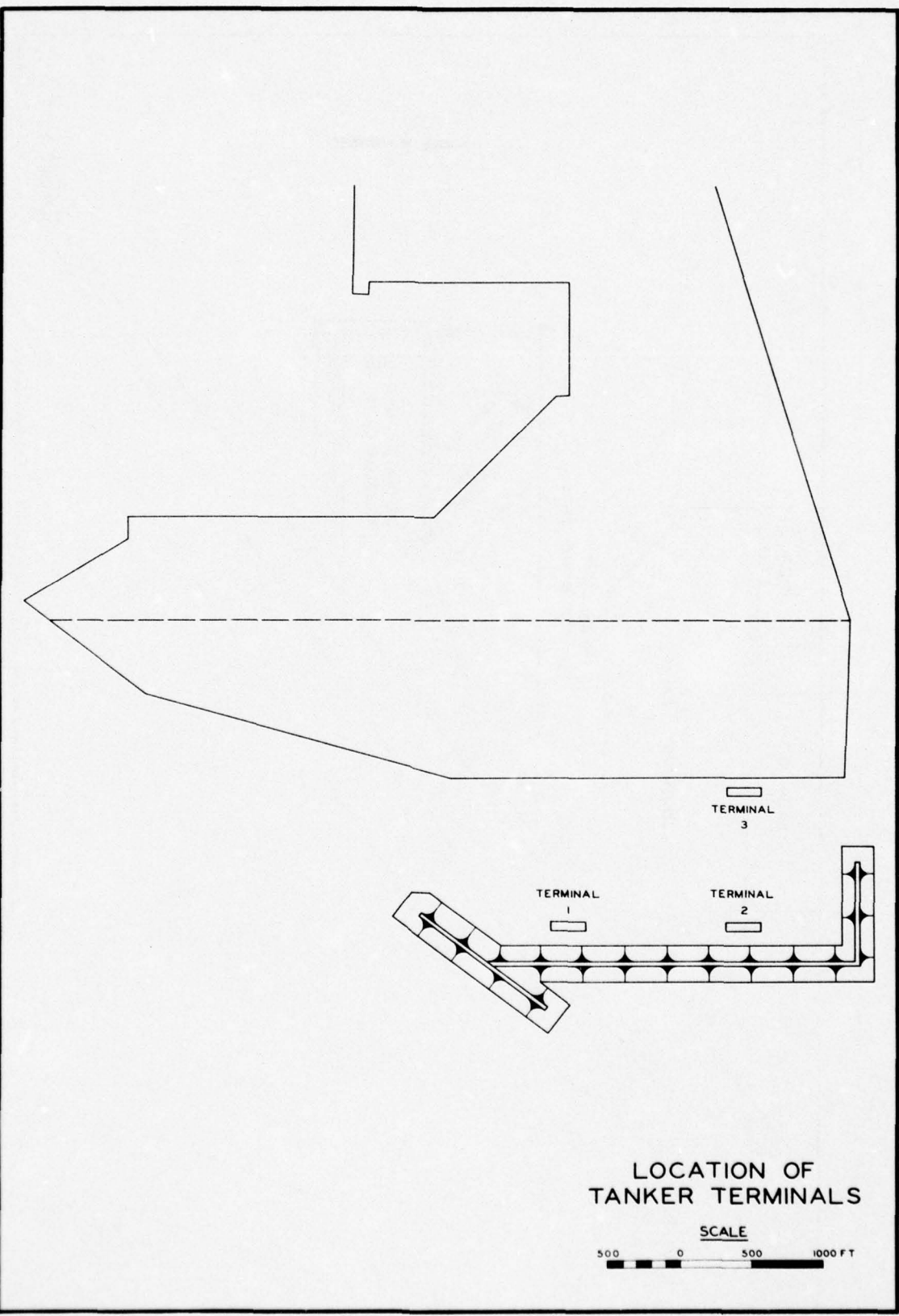
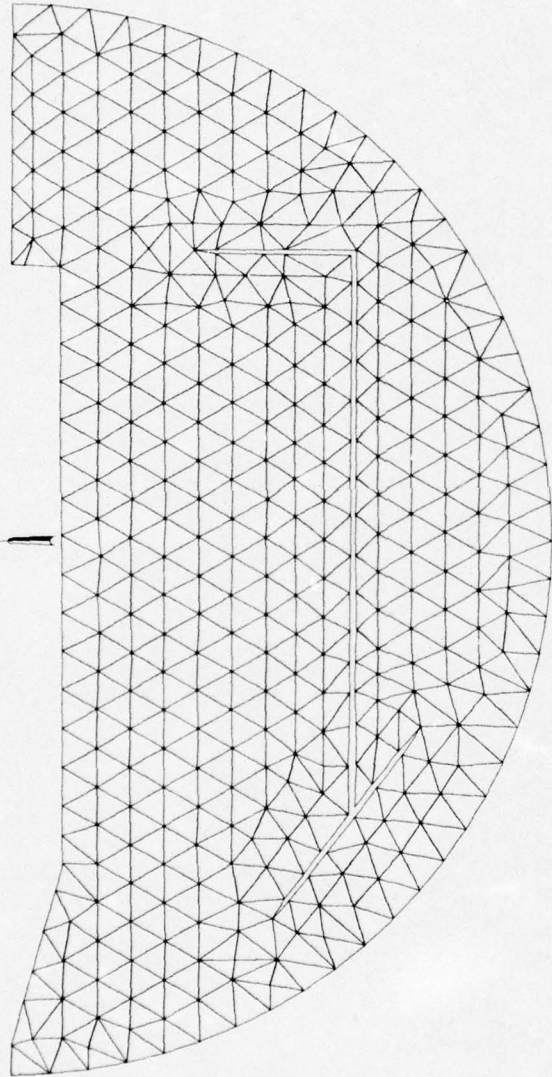


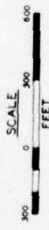
PLATE 4

FINITE ELEMENT GRID  
STFP 2 (600)  
62-FT DEPTH



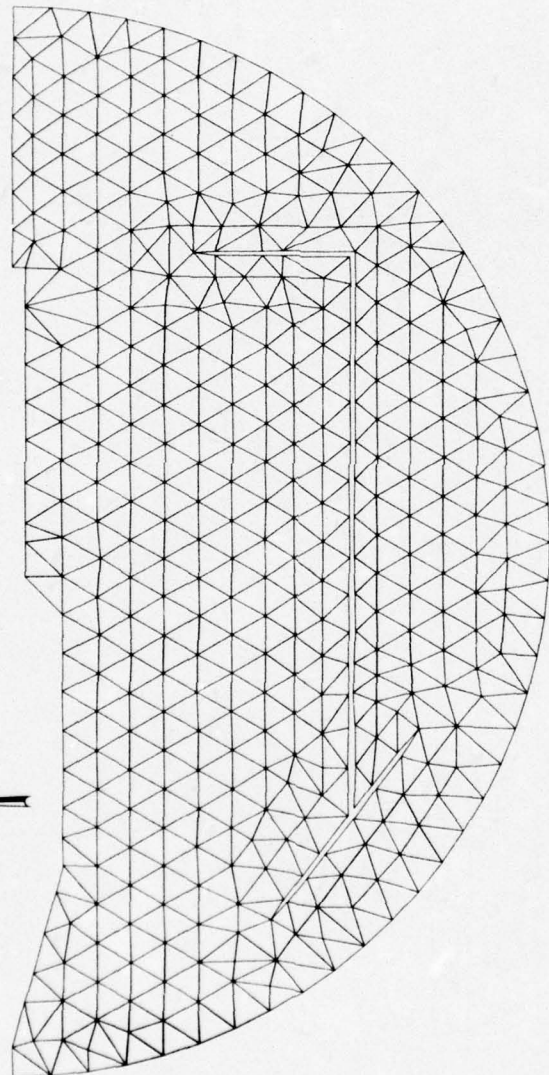
NOTE NUMBER OF NODE POINTS = 416

NUMBER OF ELEMENTS = 705



FINITE ELEMENT GRID  
STFP 2 (600)  
82-FT DEPTH

NOTE NUMBER OF NODE POINTS = 424  
NUMBER OF ELEMENTS = 721



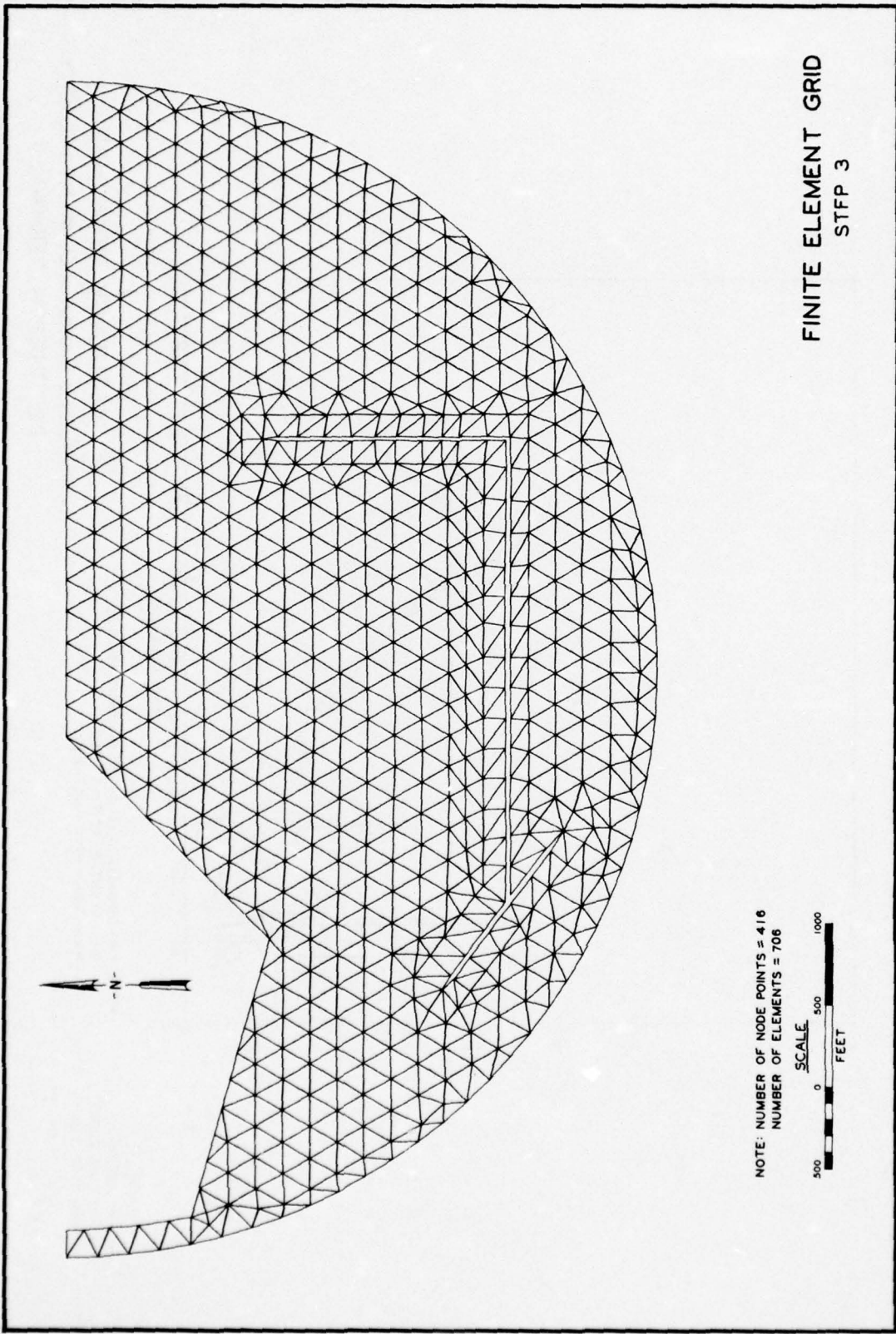


PLATE 7

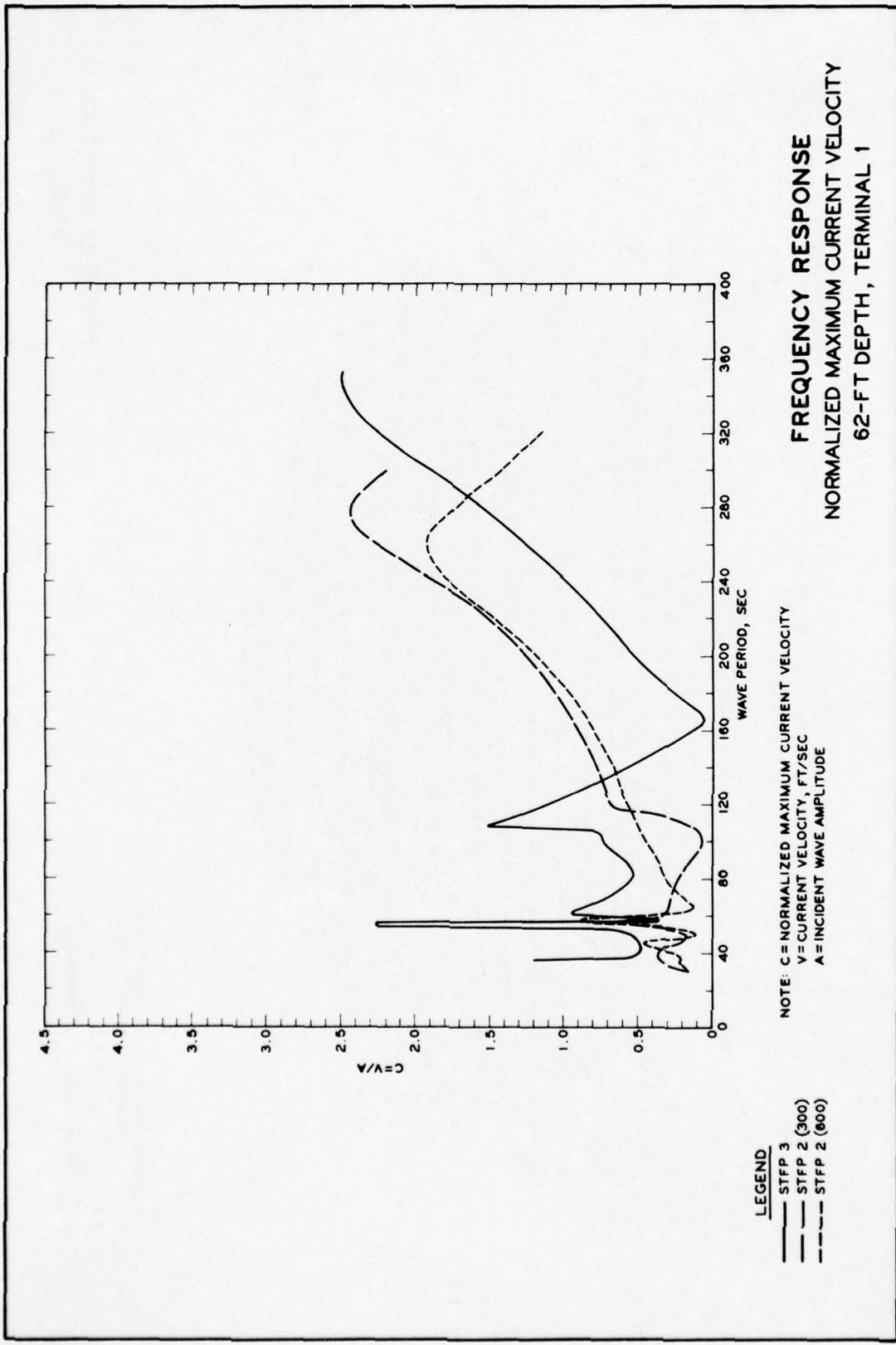
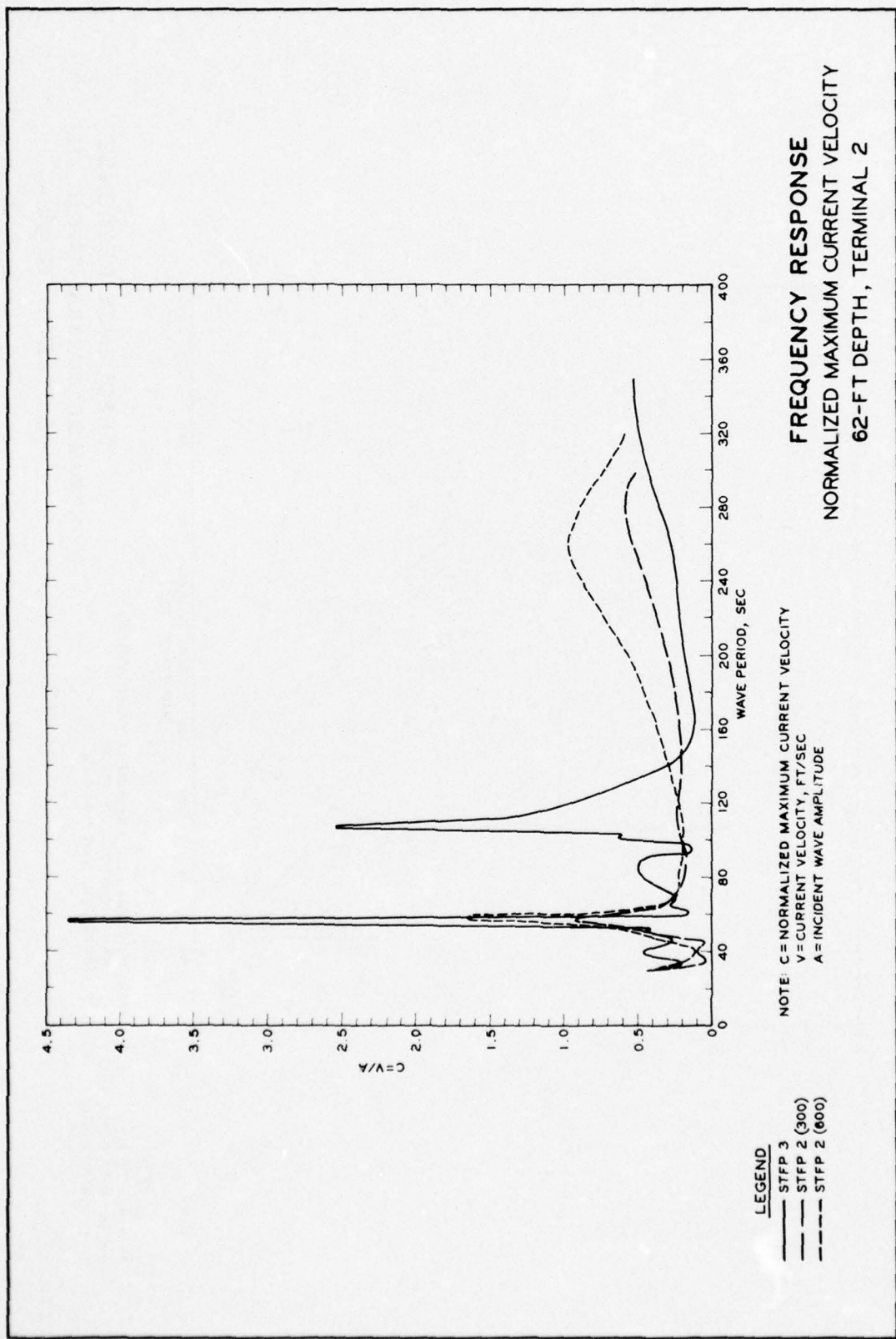


PLATE 8



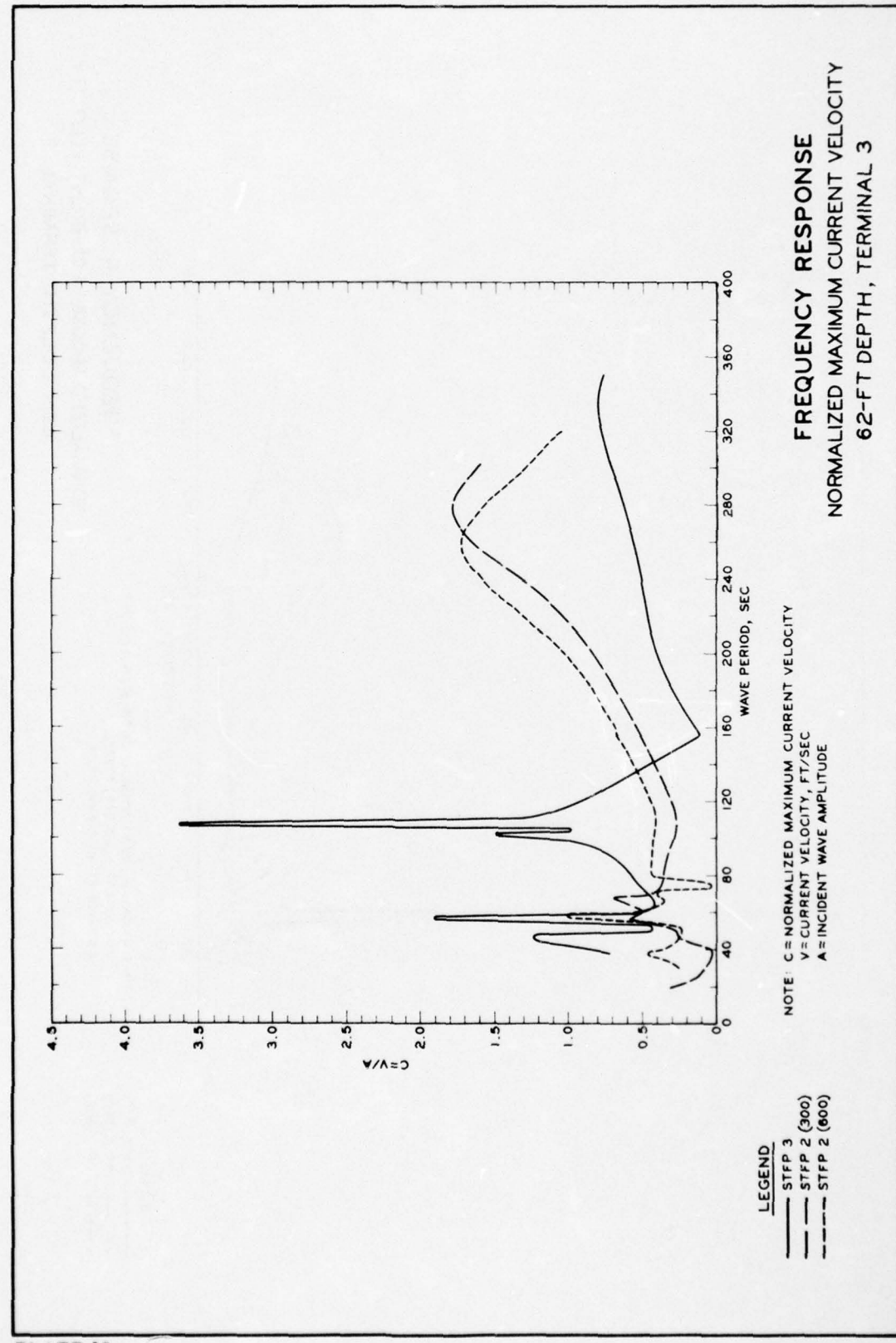


PLATE 10

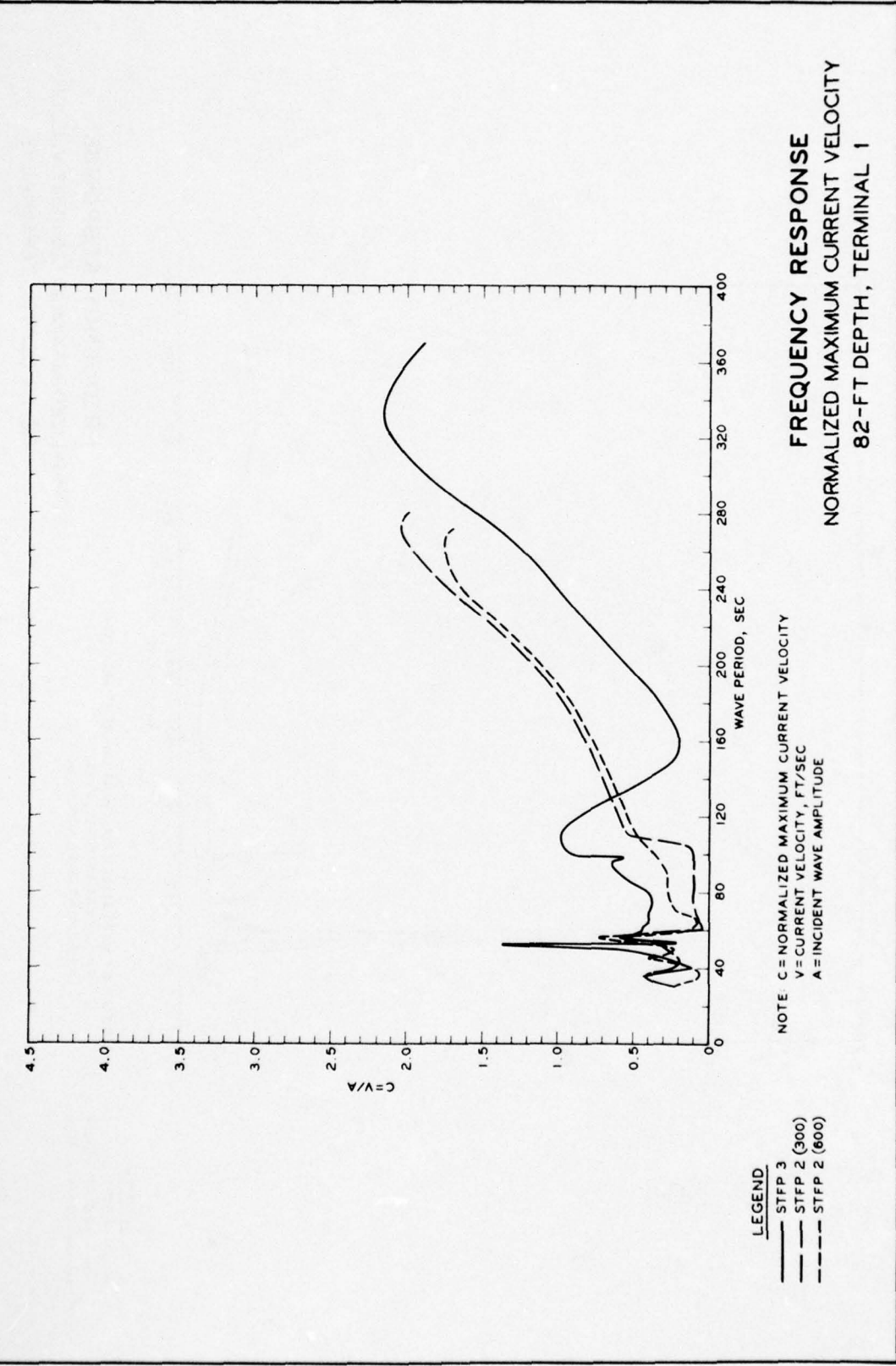


PLATE 11

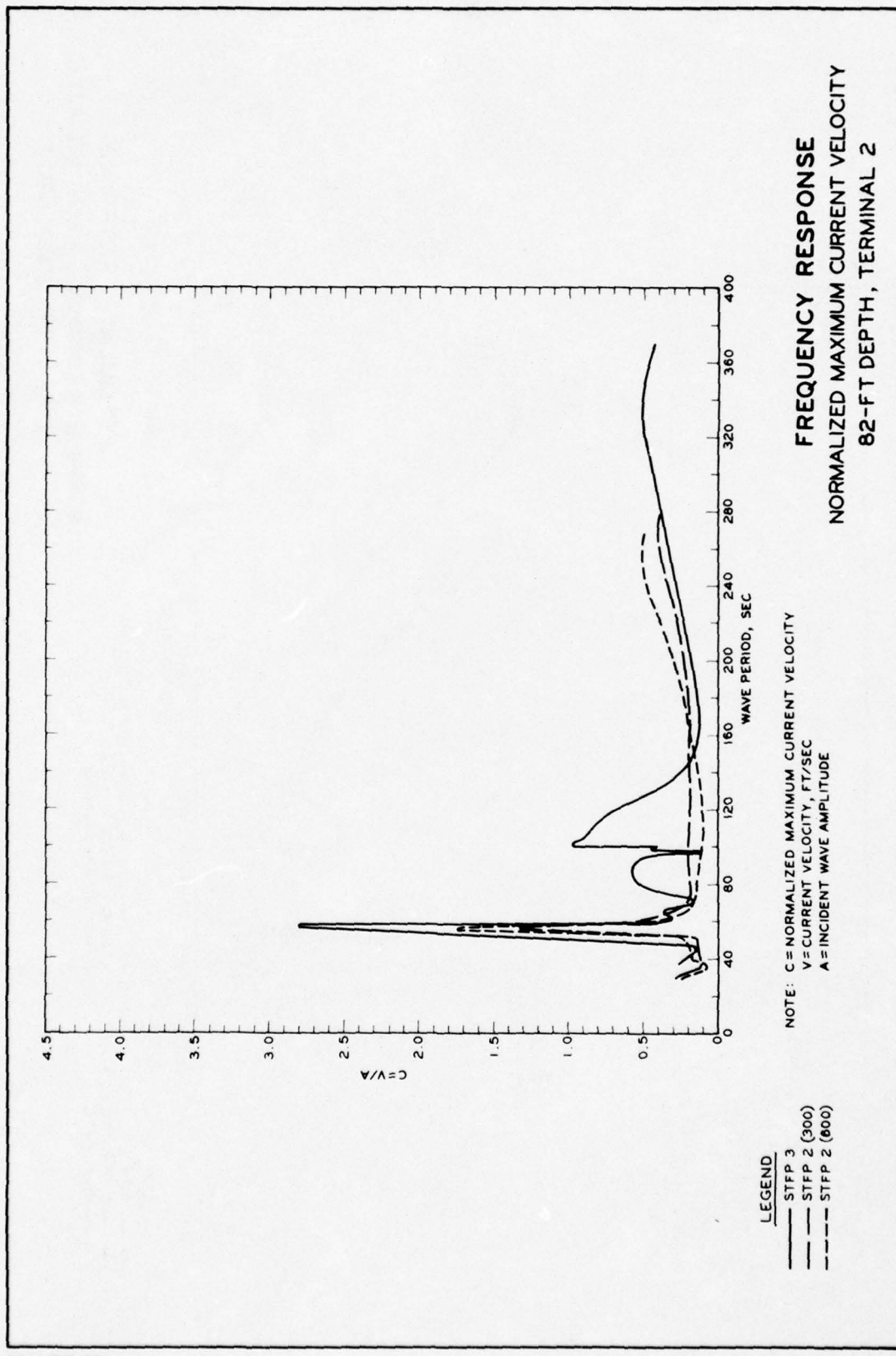
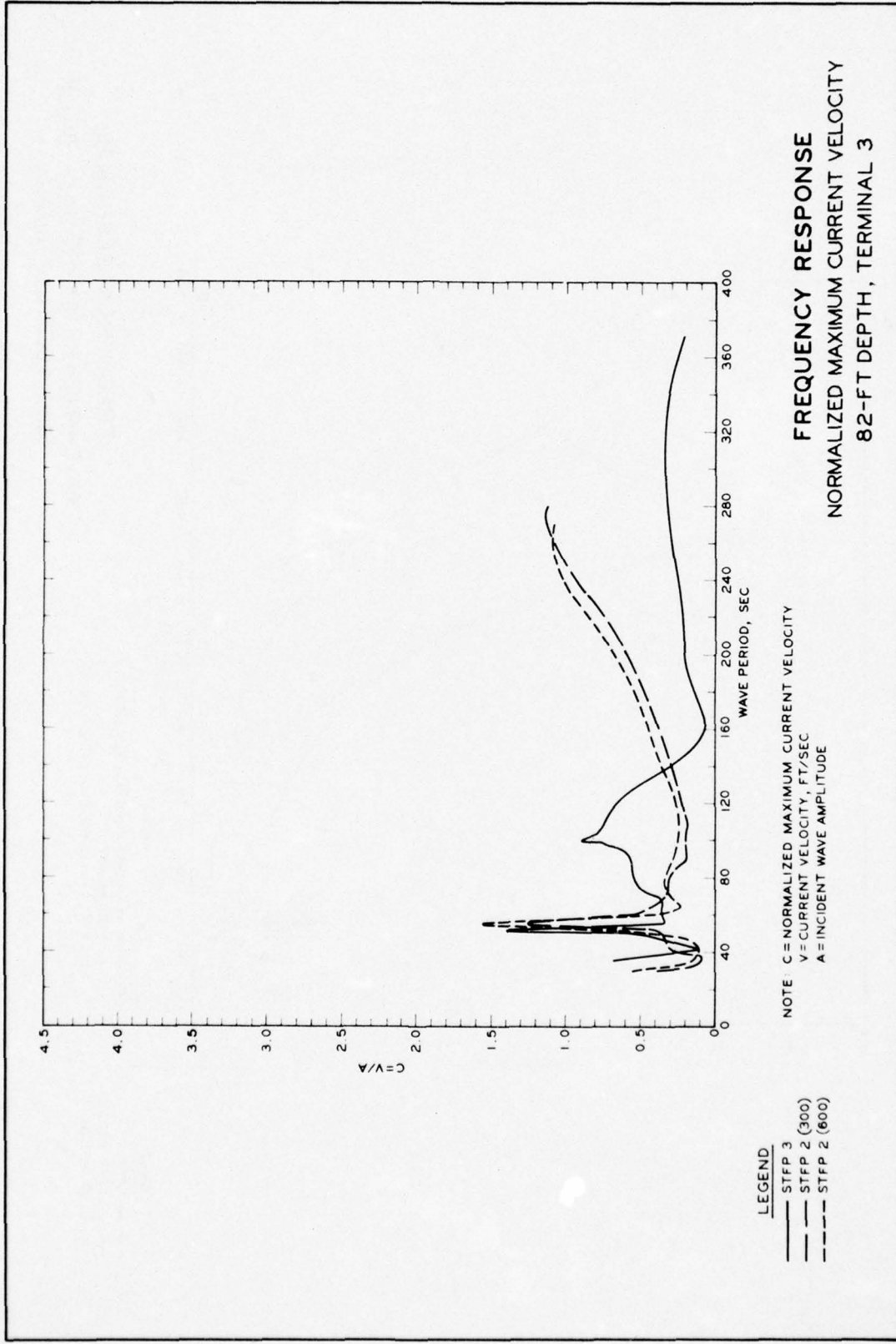


PLATE 12



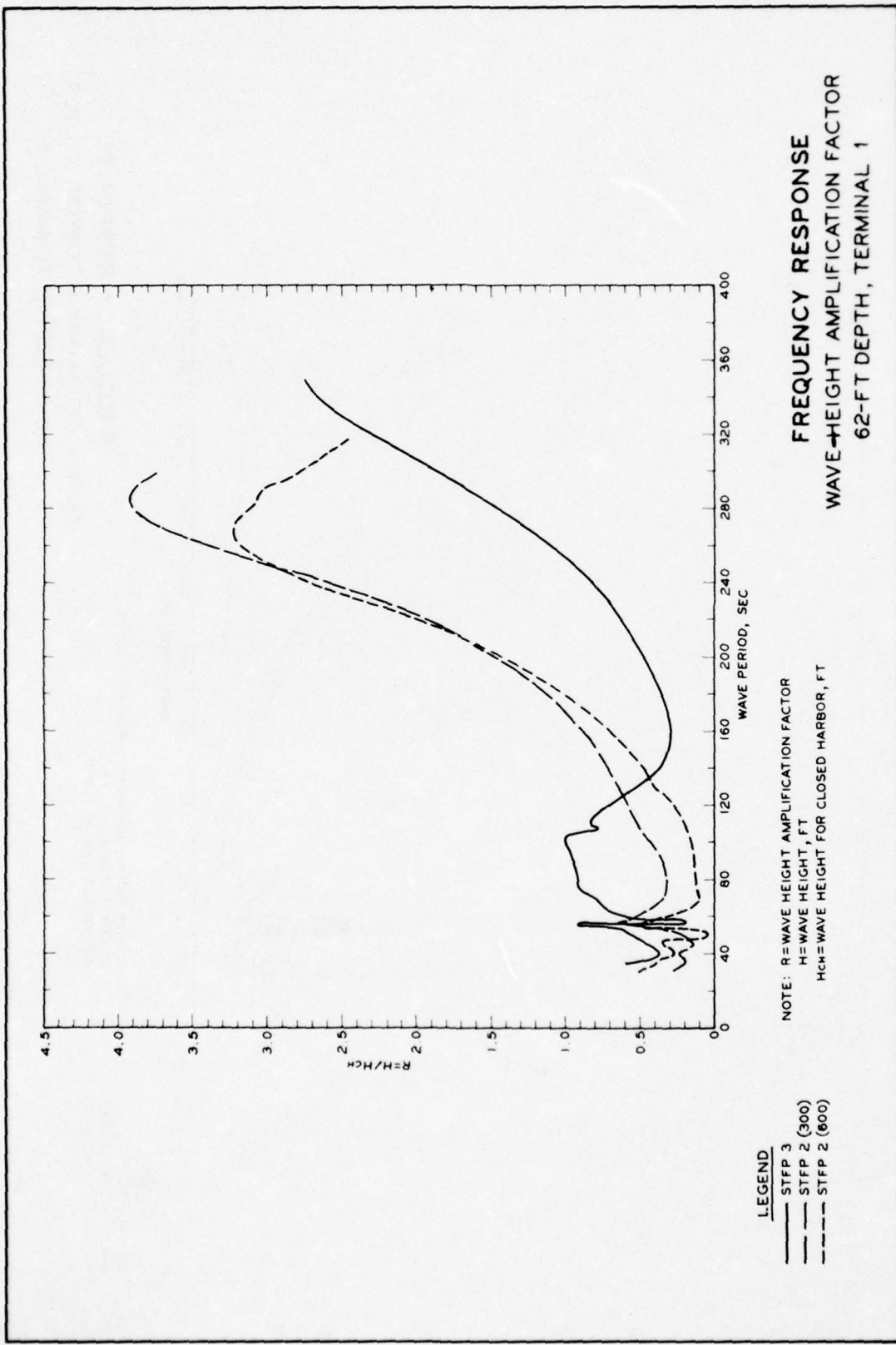
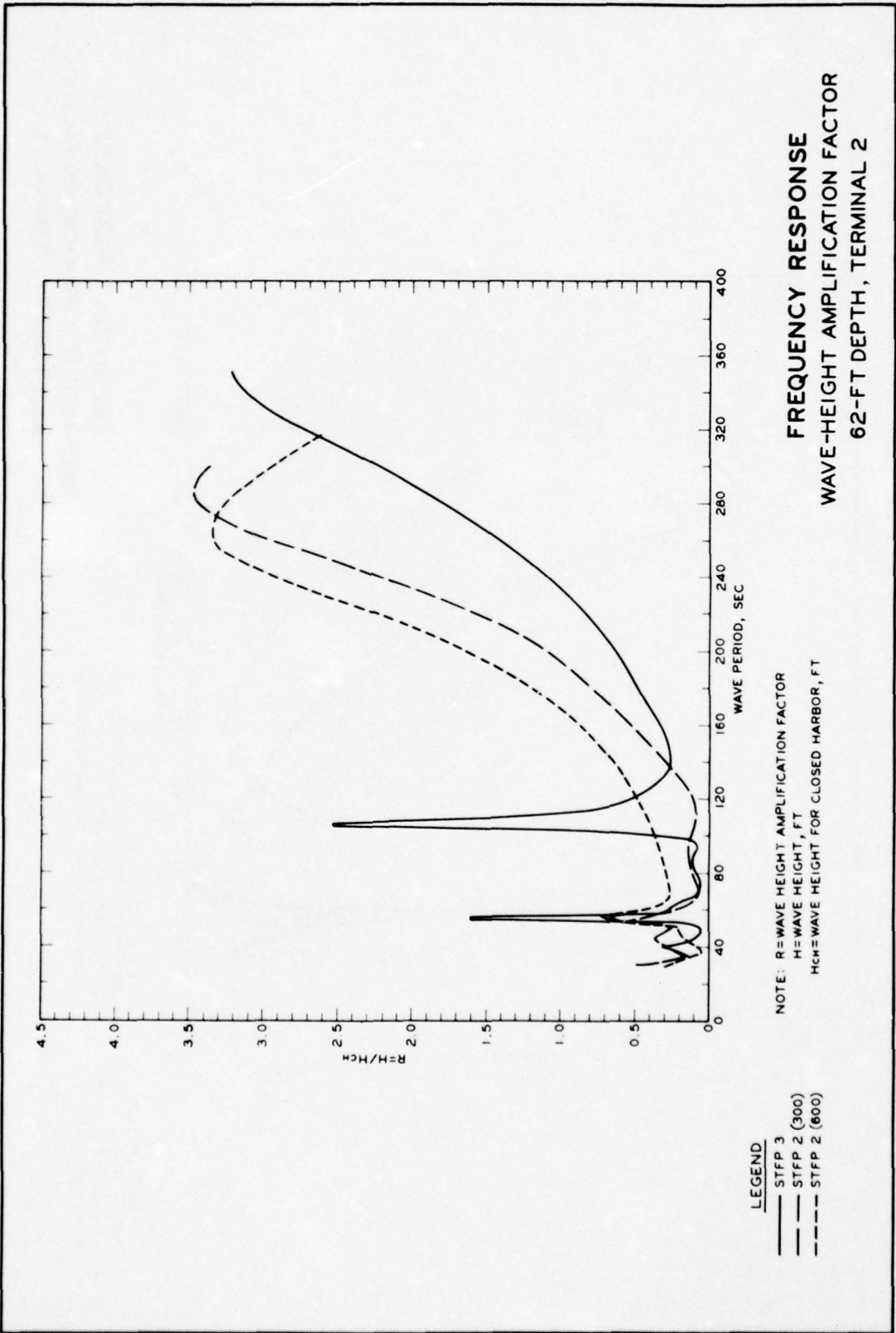


PLATE 14



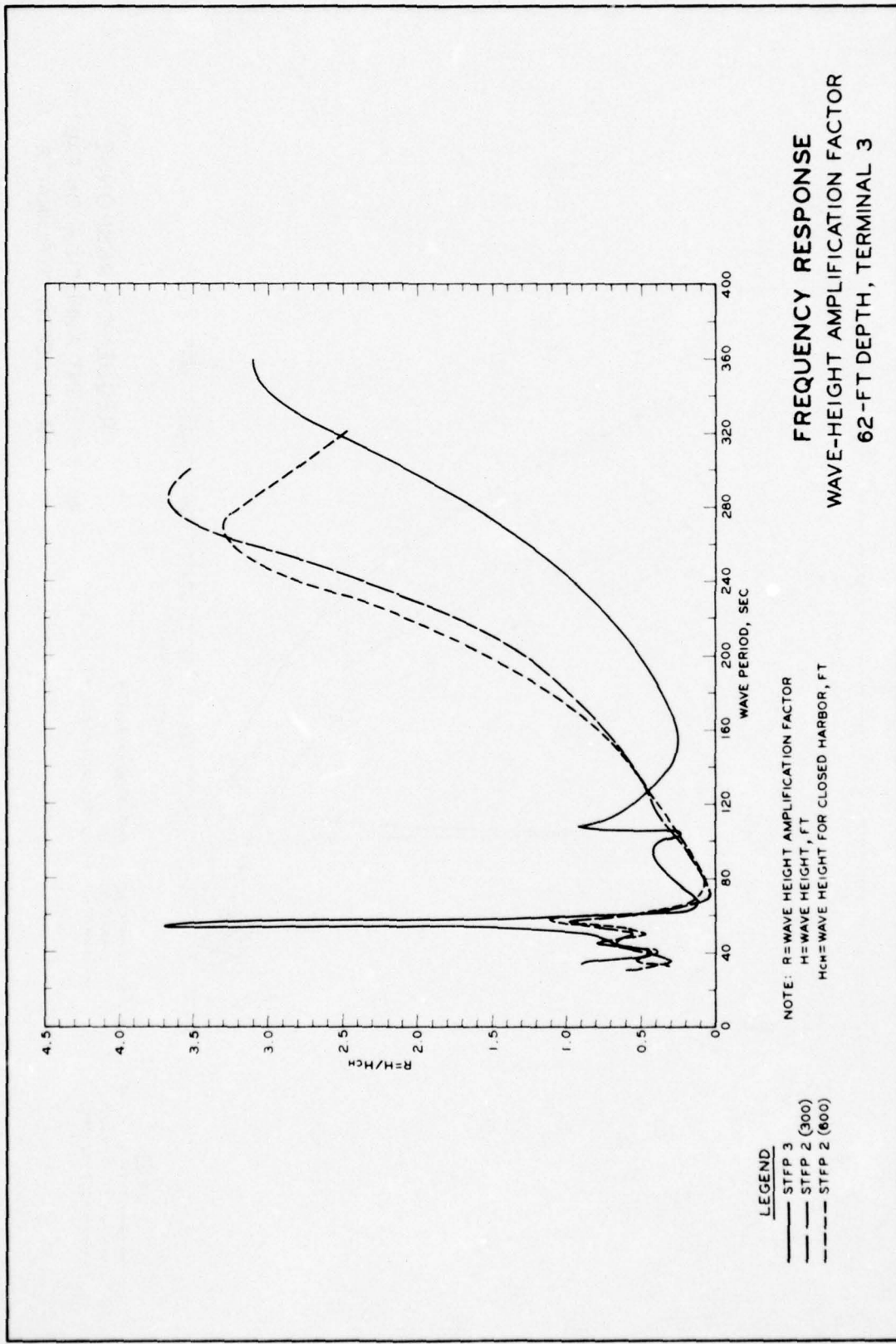
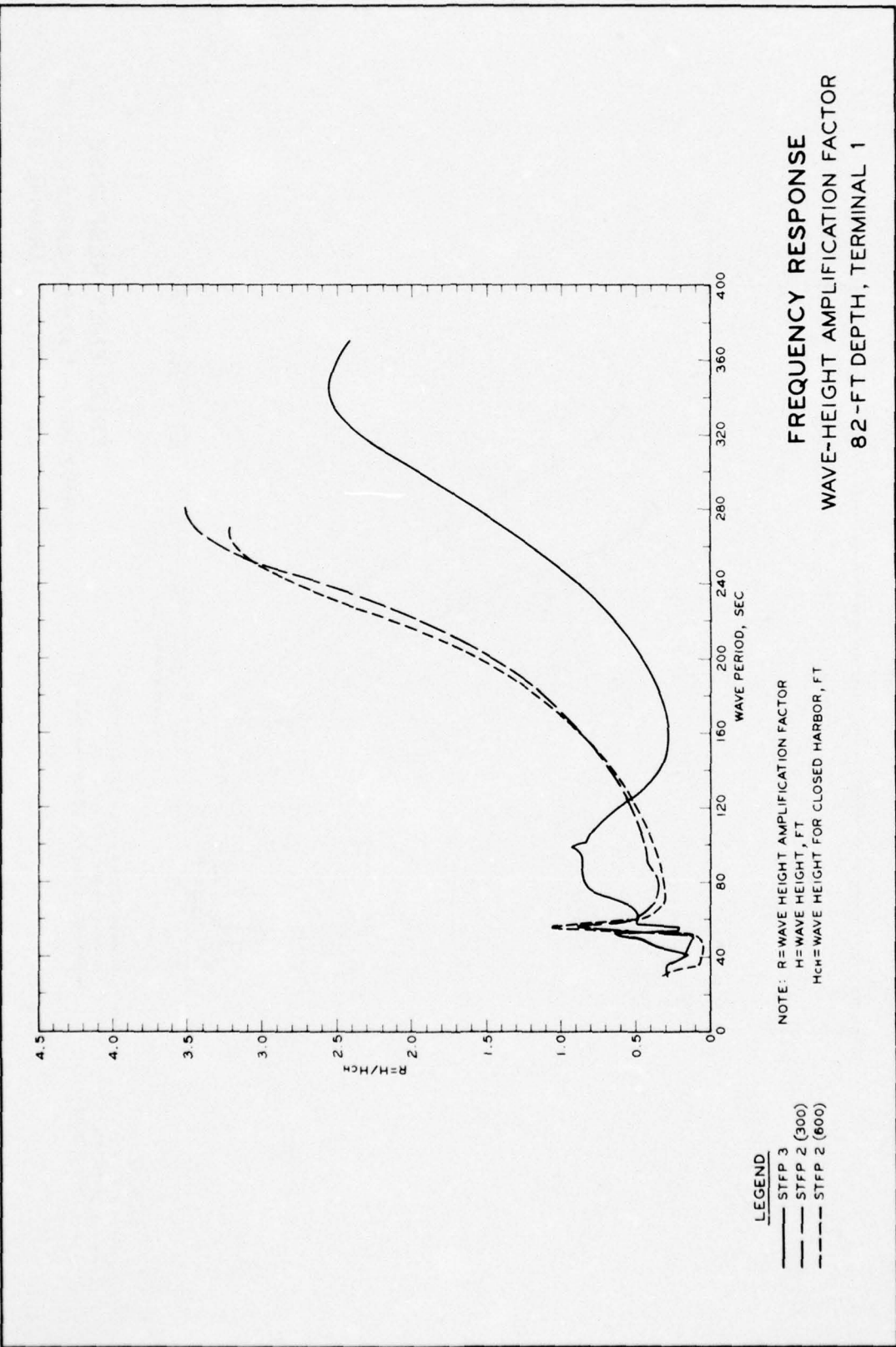


PLATE 16



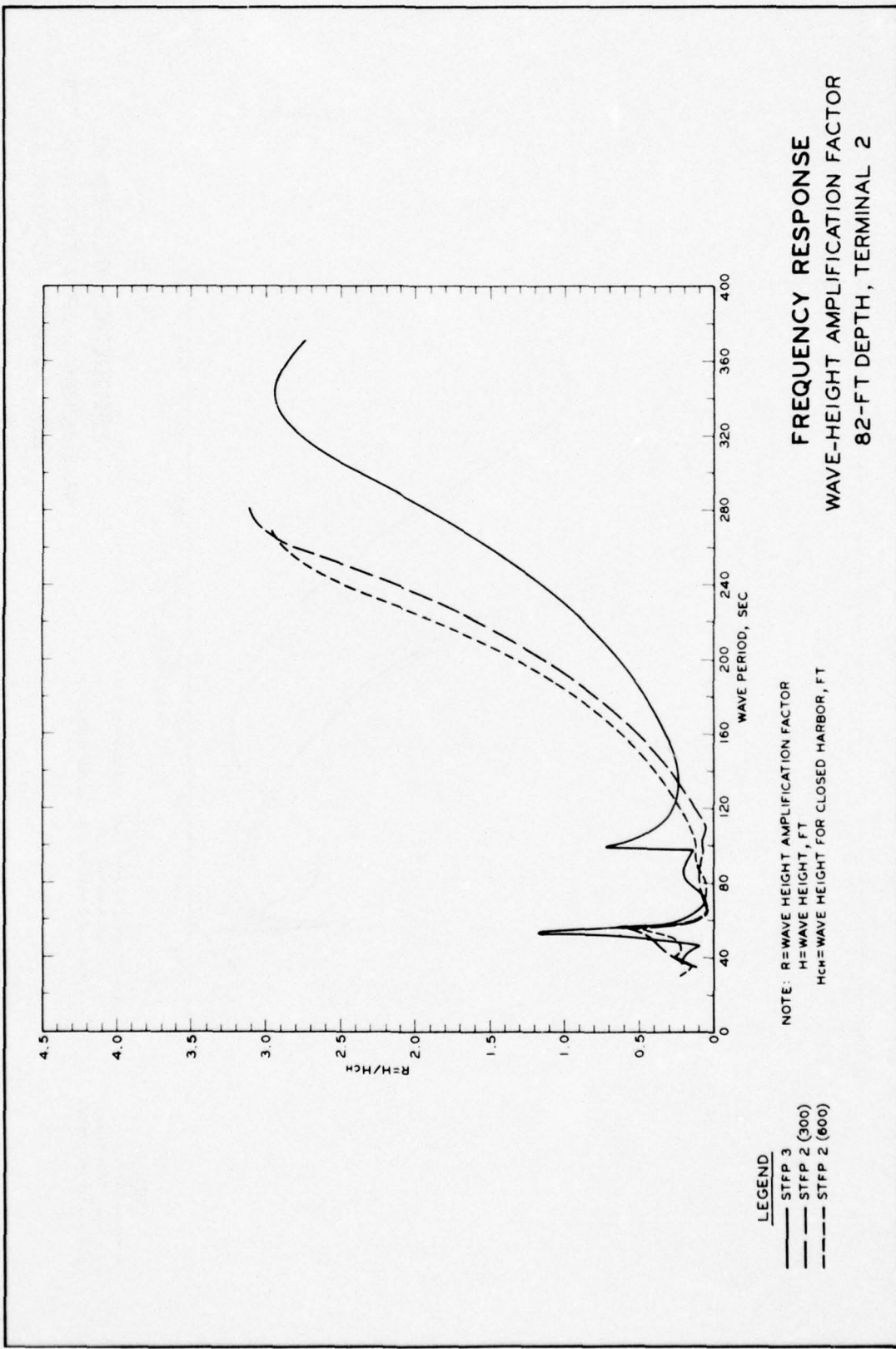
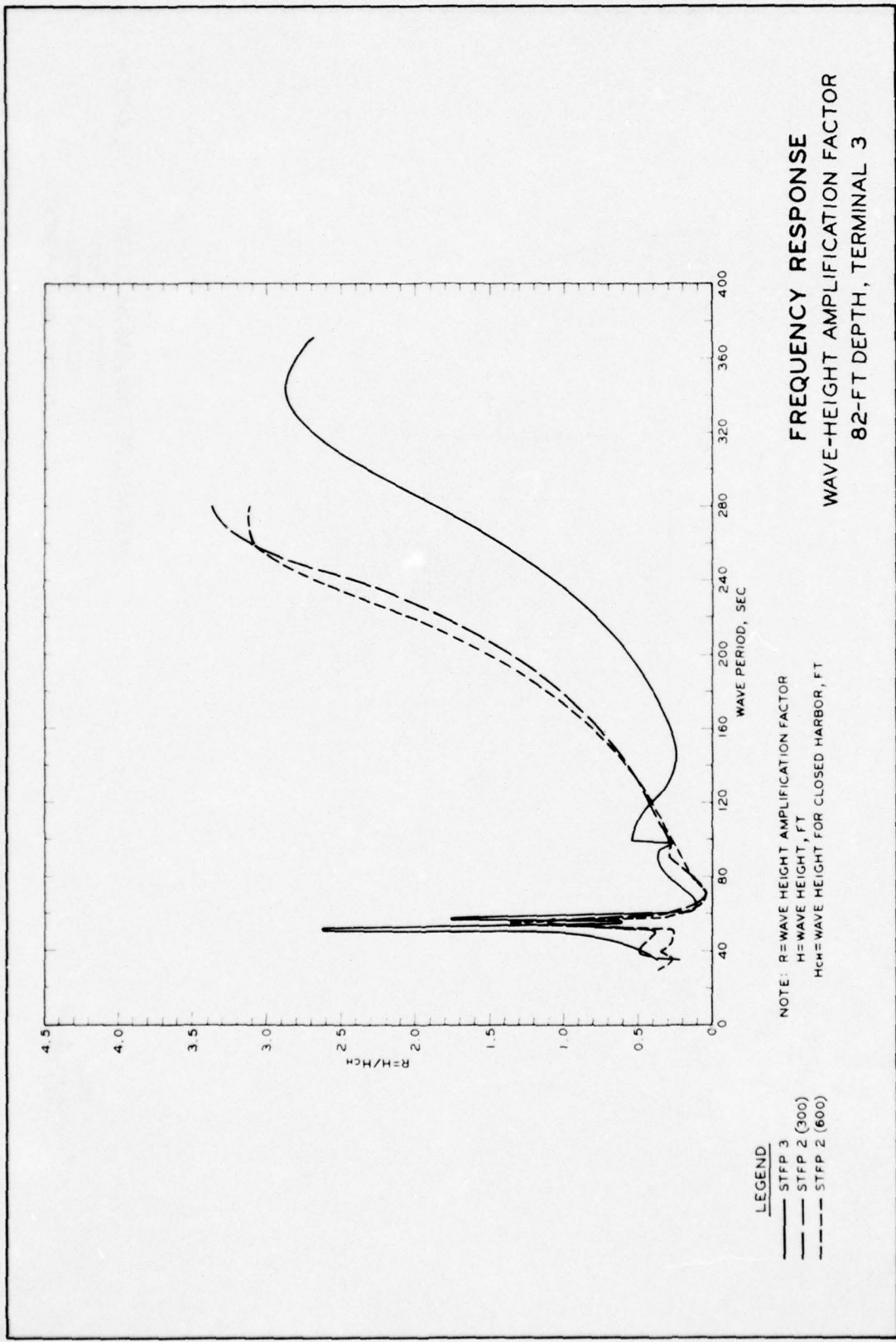
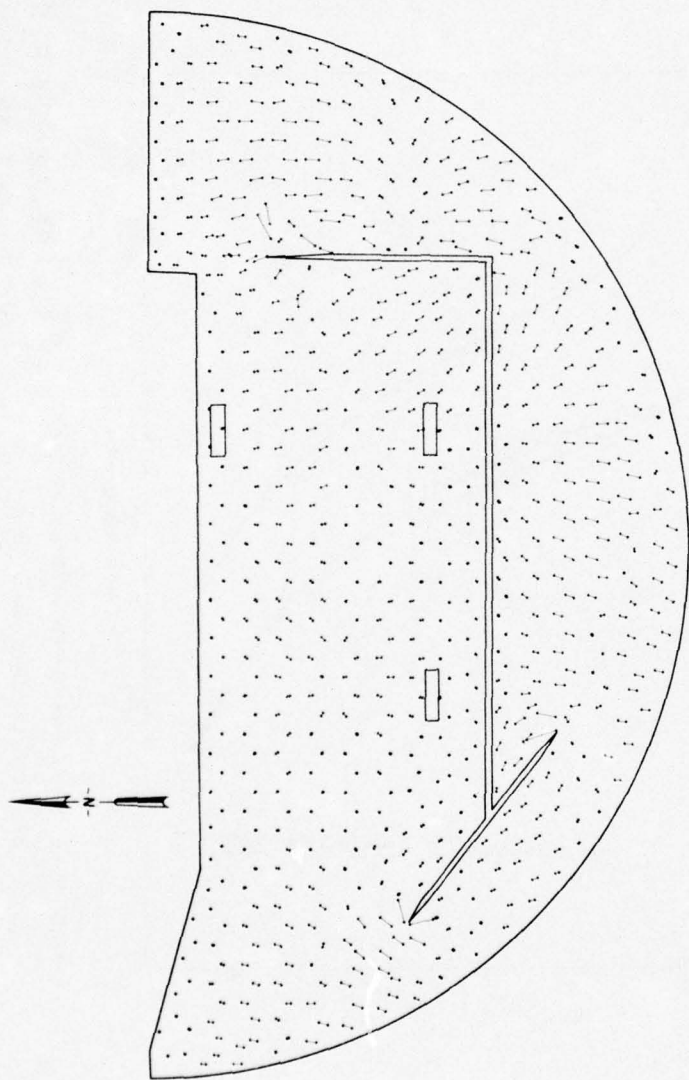


PLATE 18



NORMALIZED MAXIMUM CURRENT VELOCITY  
STFP 2 (300)  
62-FT DEPTH  
57-SEC WAVE PERIOD

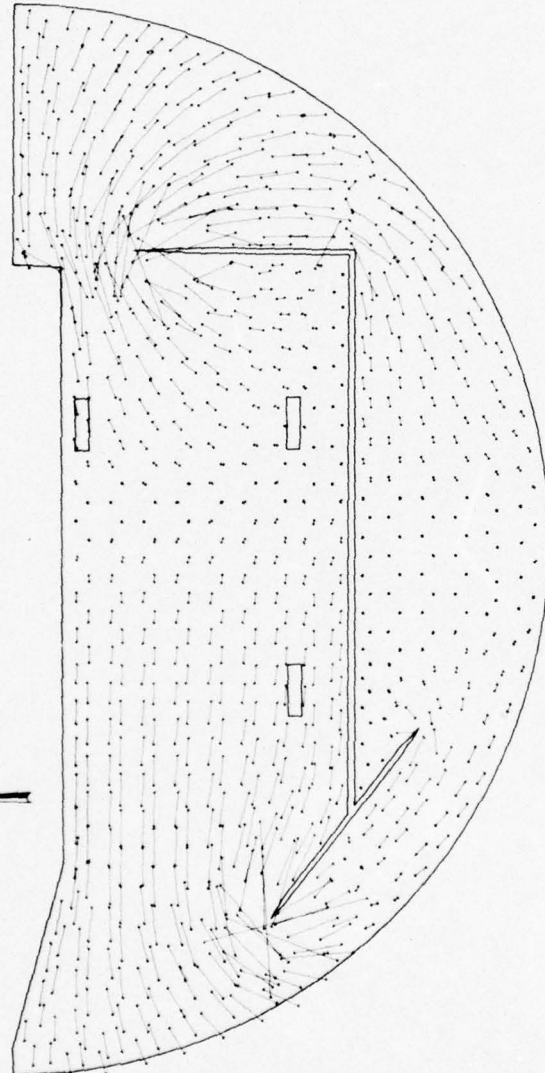
SCALE  
5 0 5 10 15  
VELOCITY FPS



NORMALIZED MAXIMUM CURRENT VELOCITY

STFP 2 (300)  
62-FT DEPTH  
280-SEC WAVE PERIOD

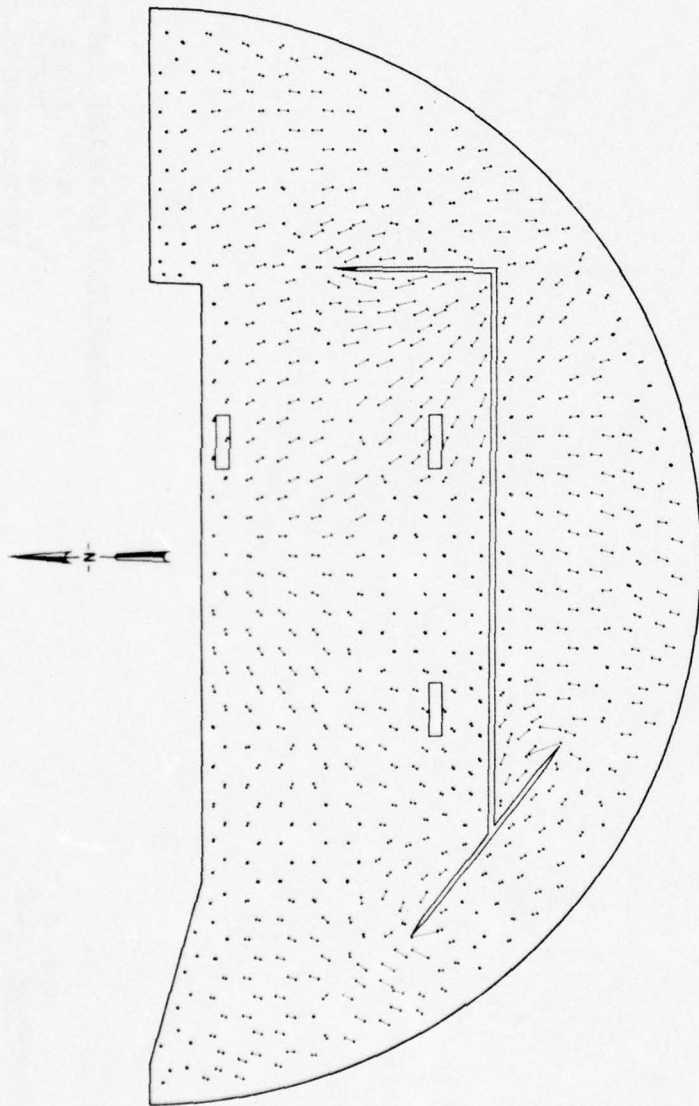
SCALE  
0 5 10 15  
VELOCITY FPS



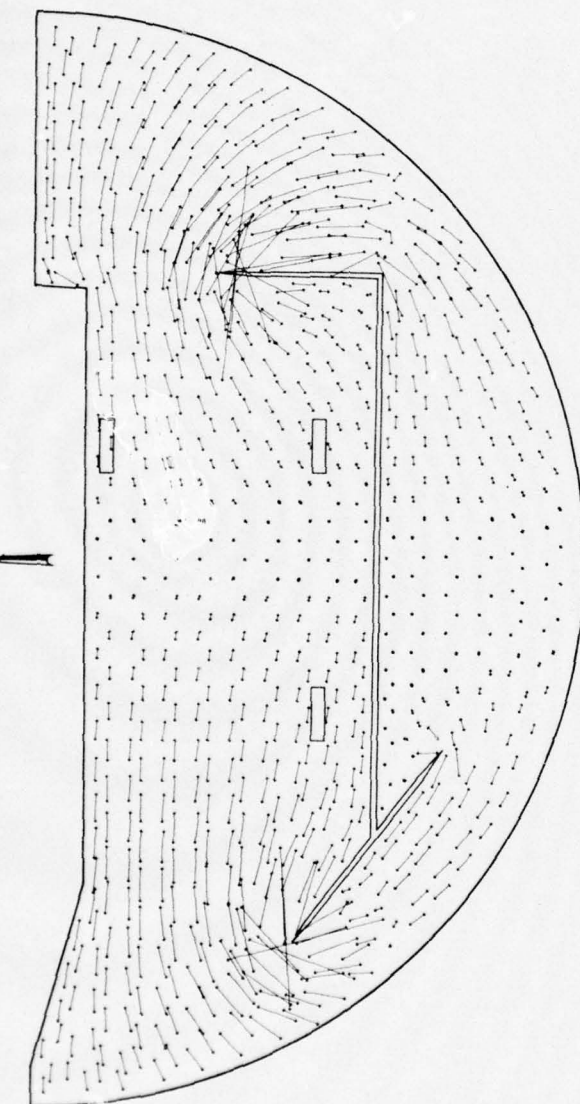
NORMALIZED MAXIMUM CURRENT VELOCITY

STFP 2 (600)  
62-FT DEPTH  
57.5-SEC WAVE PERIOD

SCALE  
0 3 6 9 12  
VELOCITY FPS



NORMALIZED MAXIMUM CURRENT VELOCITY  
STFP 2 (600)  
62-FT DEPTH  
260-SEC WAVE PERIOD



NORMALIZED MAXIMUM CURRENT VELOCITY  
STFP 3  
62-FT DEPTH  
5.5-SEC WAVE PERIOD

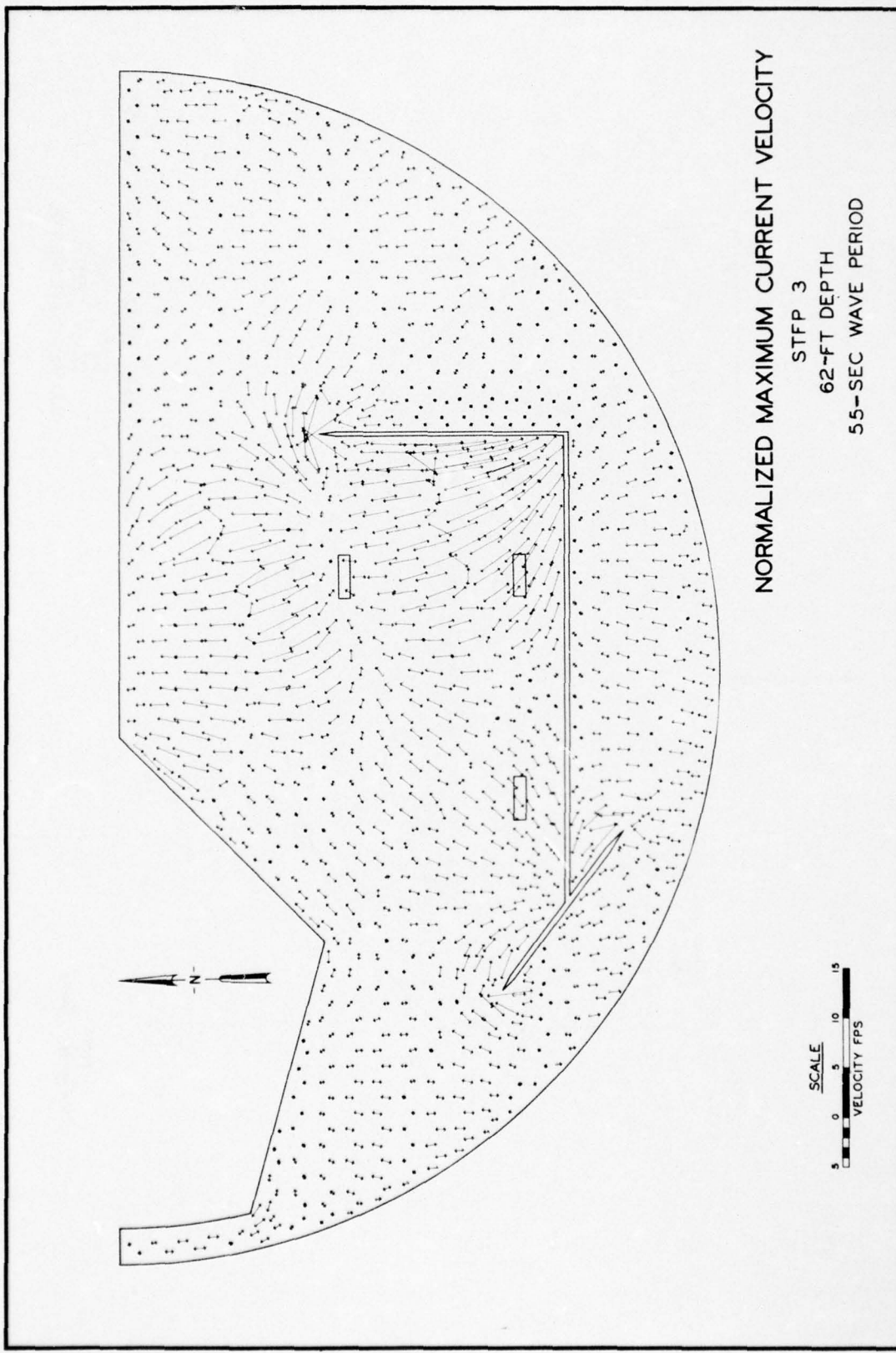


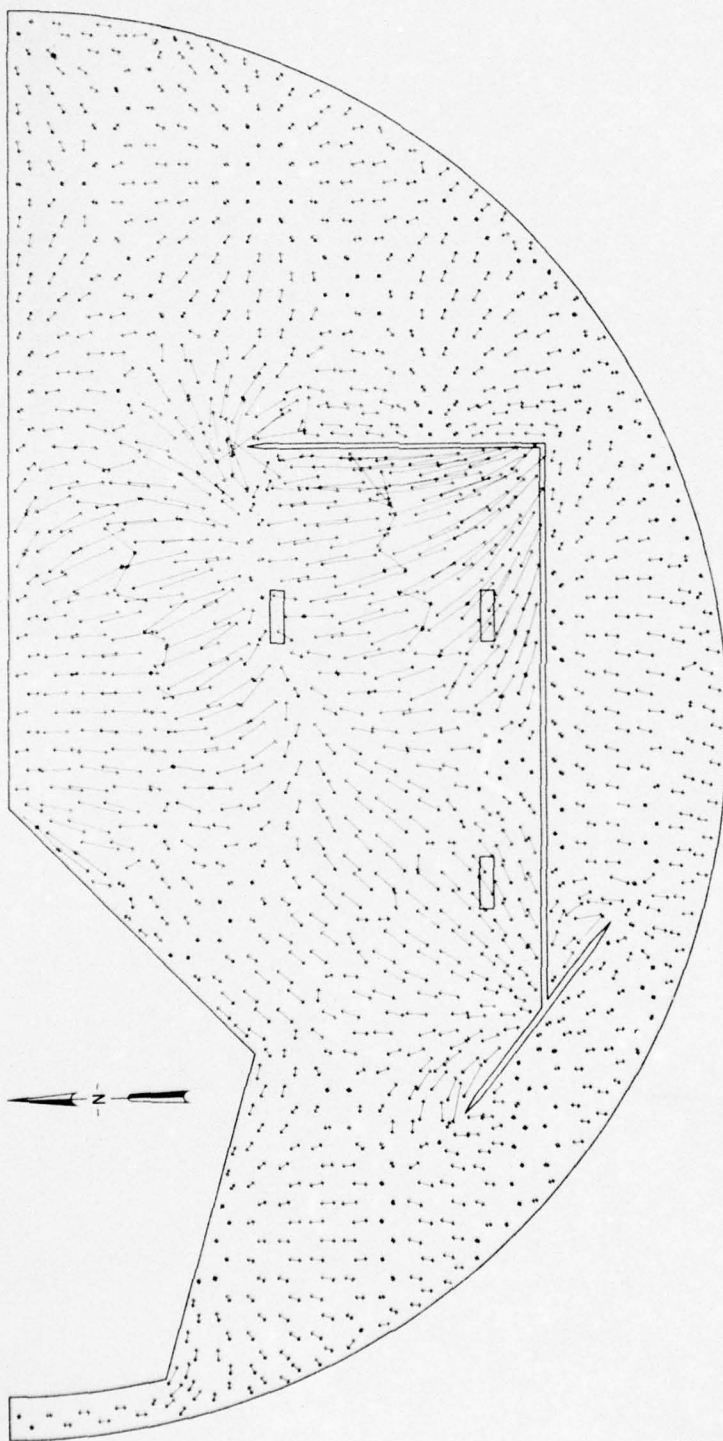
PLATE 24

NORMALIZED MAXIMUM CURRENT VELOCITY

STFP 3

62-FT DEPTH

55.5-SEC WAVE PERIOD

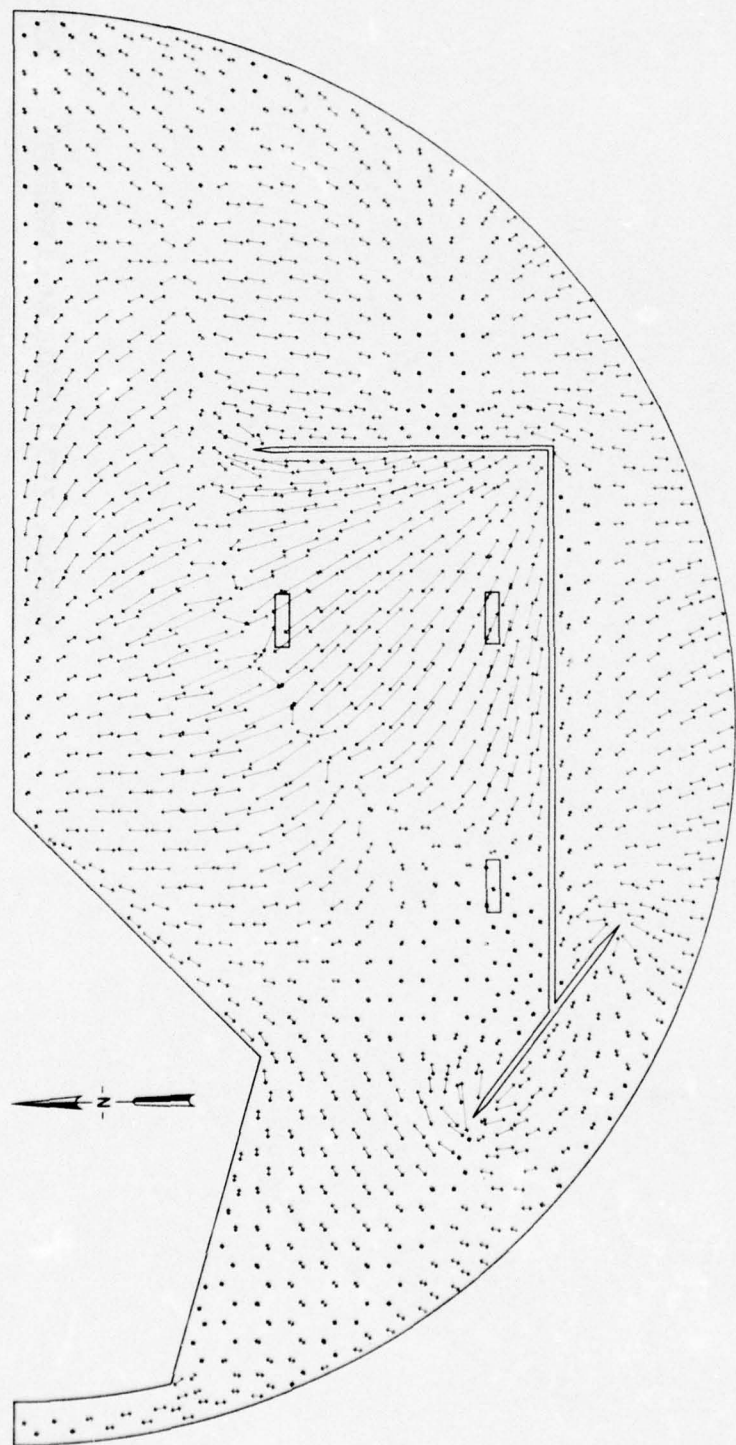


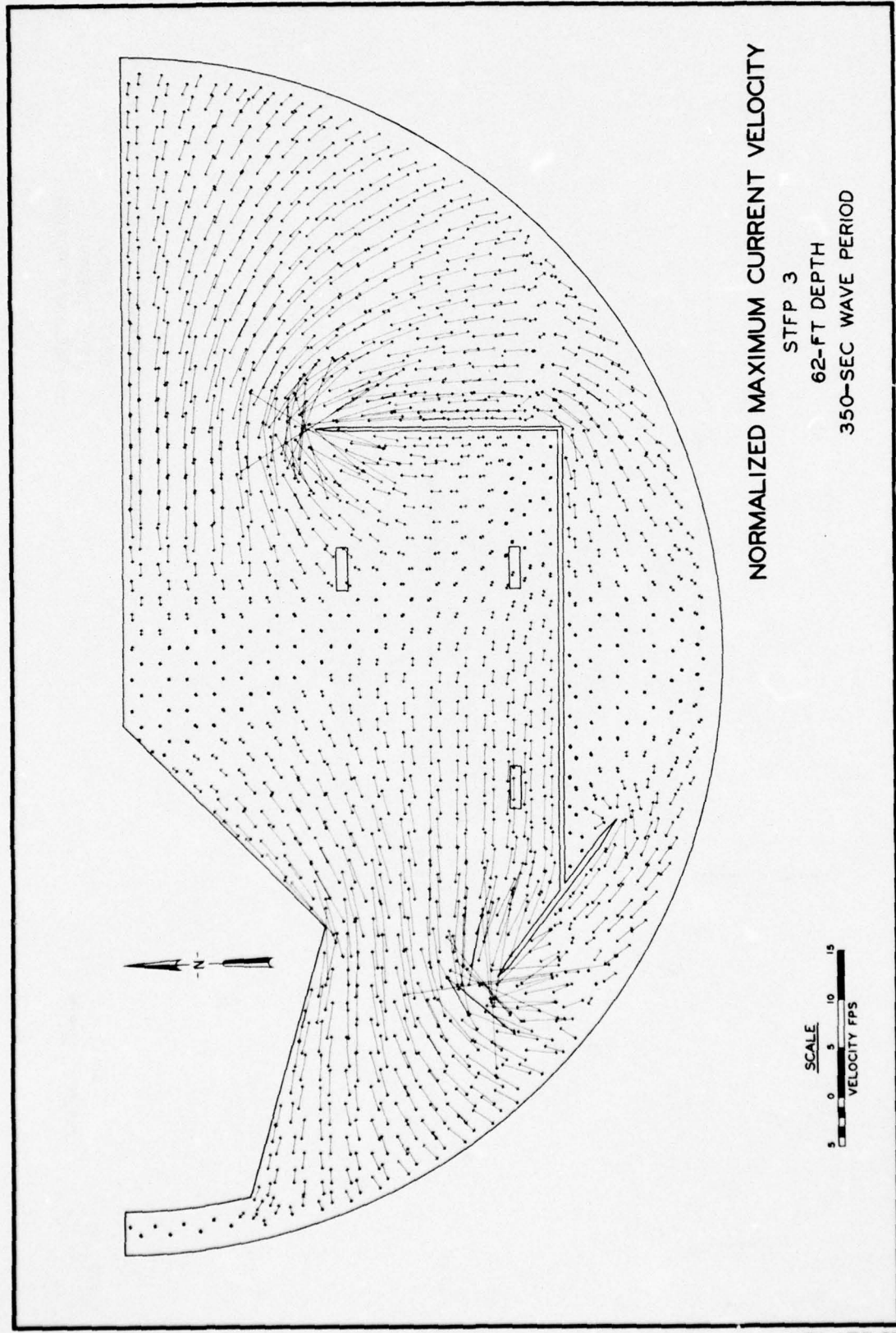
NORMALIZED MAXIMUM CURRENT VELOCITY

STFP 3

62-FT DEPTH

106-SEC WAVE PERIOD





NORMALIZED MAXIMUM CURRENT VELOCITY  
STFP 2 (300)  
82 FT DEPTH  
56 SEC WAVE PERIOD

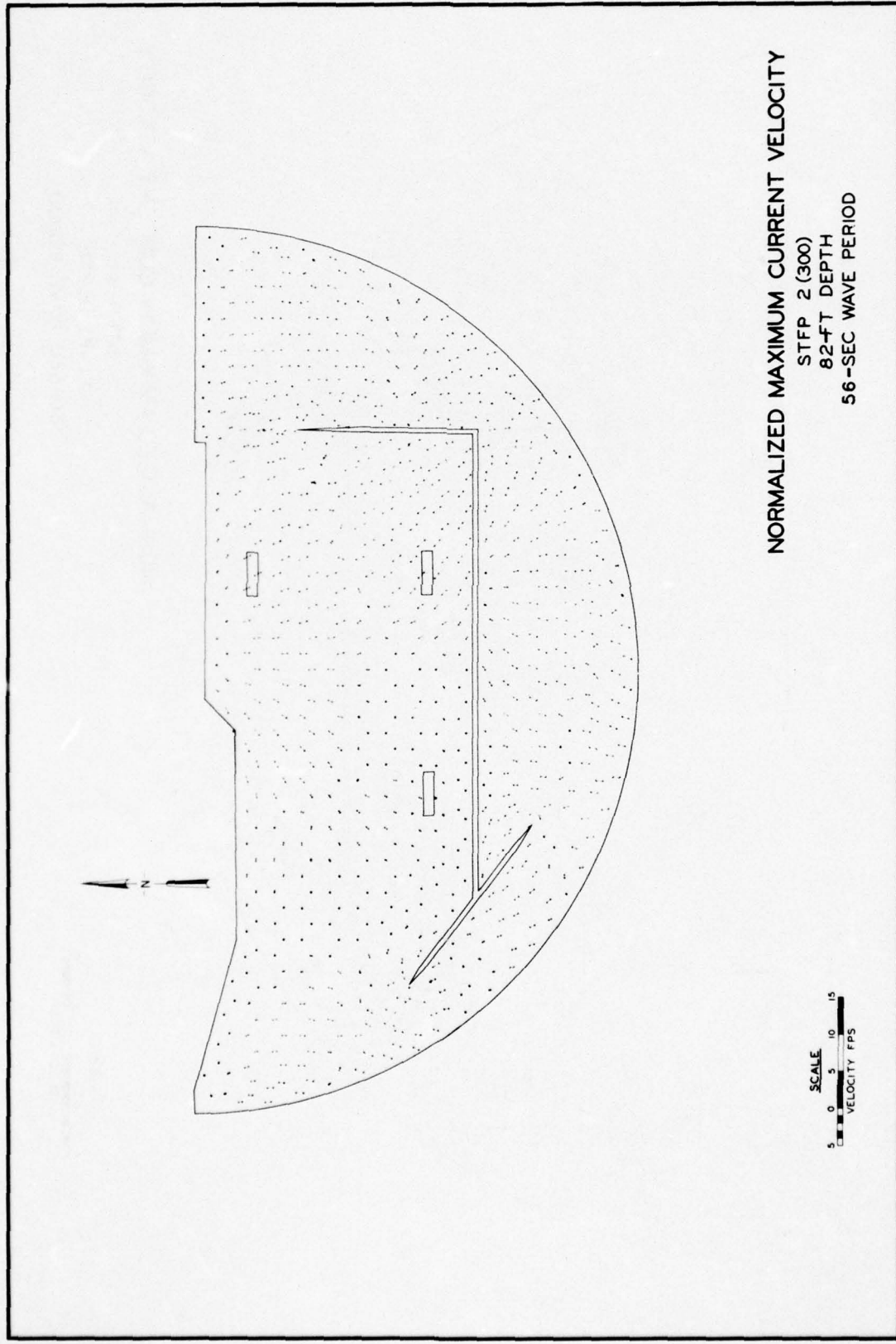
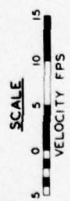
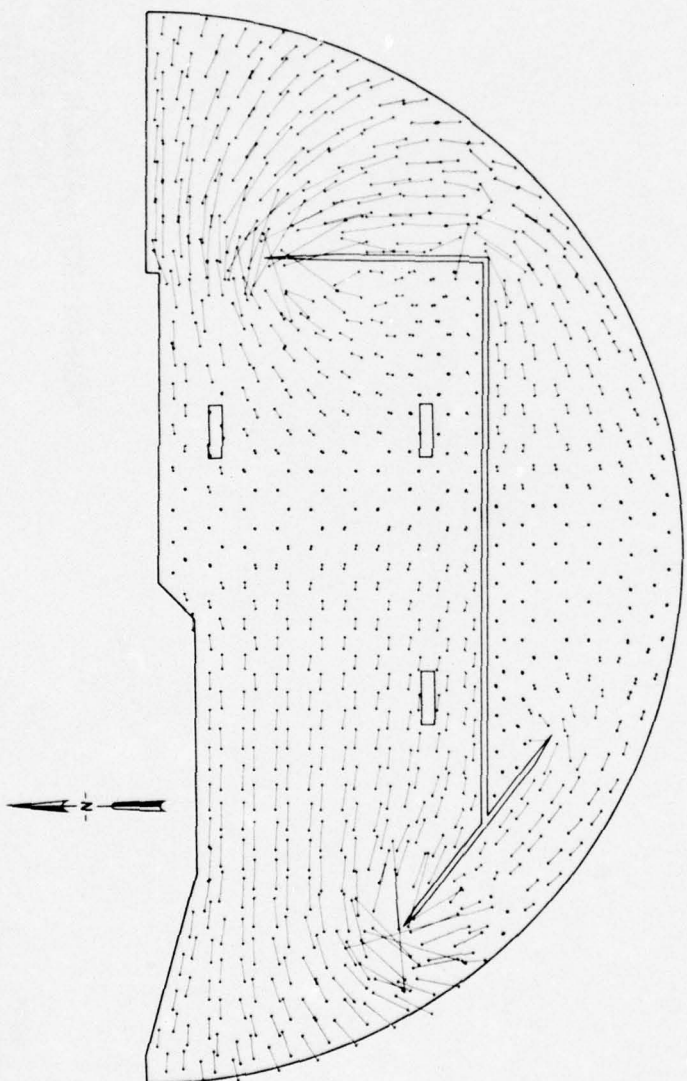
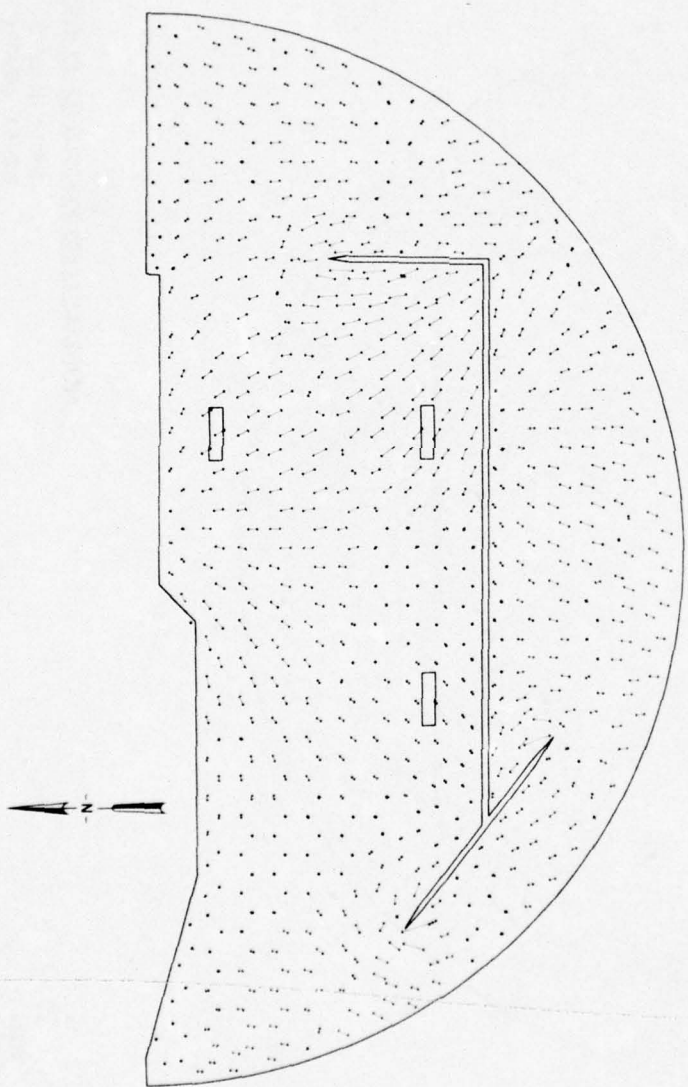


PLATE 28

NORMALIZED MAXIMUM CURRENT VELOCITY  
STFP 2(300)  
82-FT DEPTH  
270-SEC WAVE PERIOD

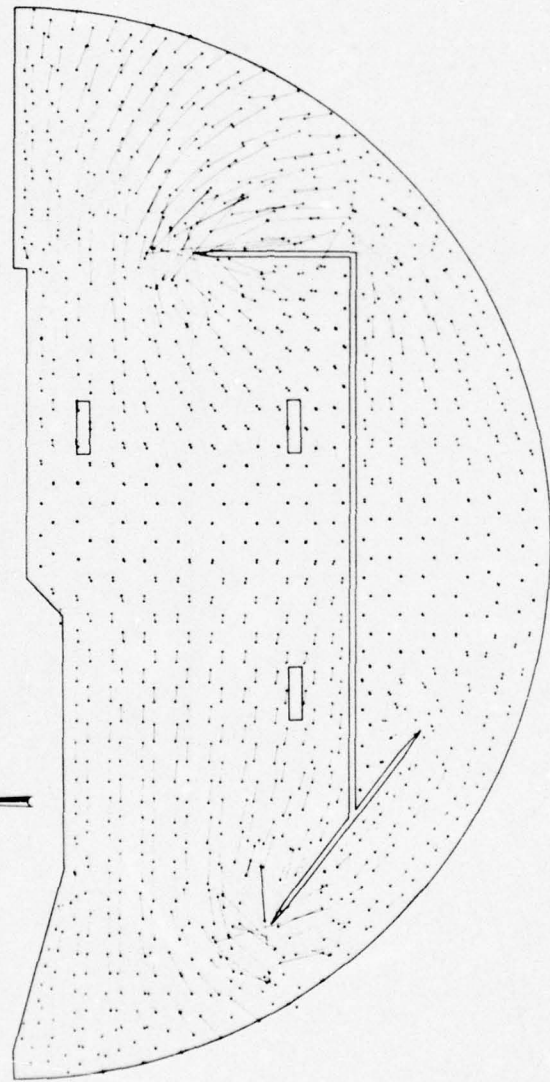


NORMALIZED MAXIMUM CURRENT VELOCITY  
STFP 2 (600)  
82-FT DEPTH  
55.5-SEC WAVE PERIOD

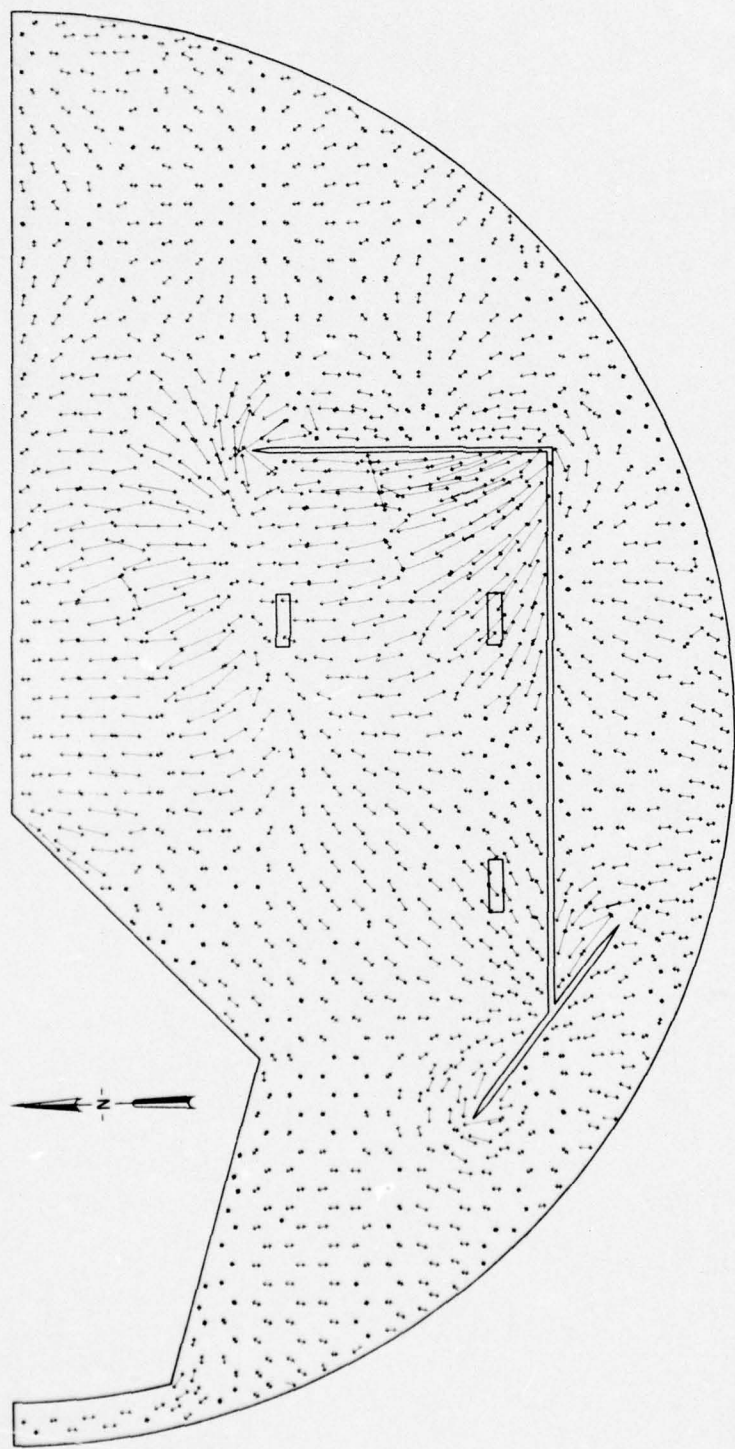


NORMALIZED MAXIMUM CURRENT VELOCITY  
STFP 2 (600)  
82-FT DEPTH  
255-SEC WAVE PERIOD

SCALE  
VELOCITY FPS  
5 0 5 10 15



NORMALIZED MAXIMUM CURRENT VELOCITY  
STFP 3  
82-FT DEPTH  
52-SEC WAVE PERIOD

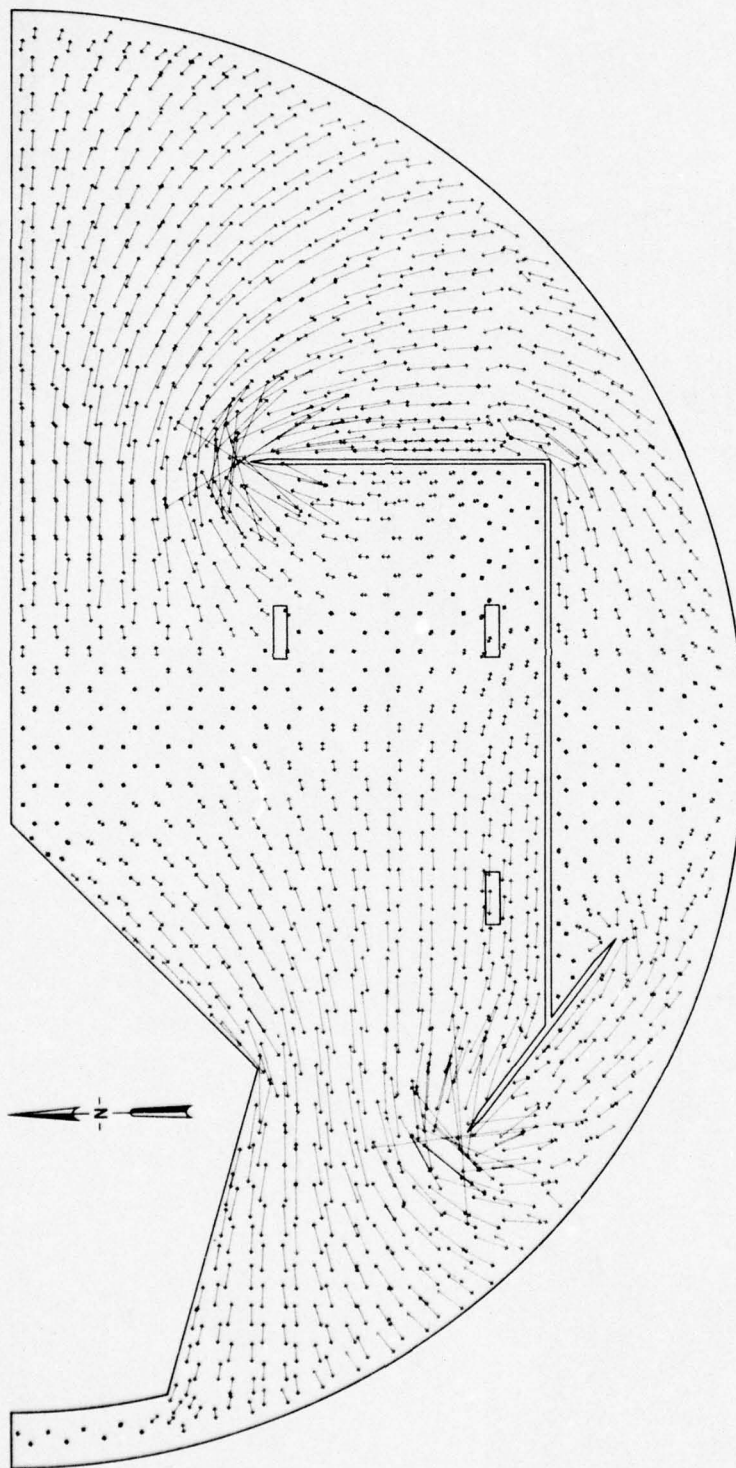


NORMALIZED MAXIMUM CURRENT VELOCITY

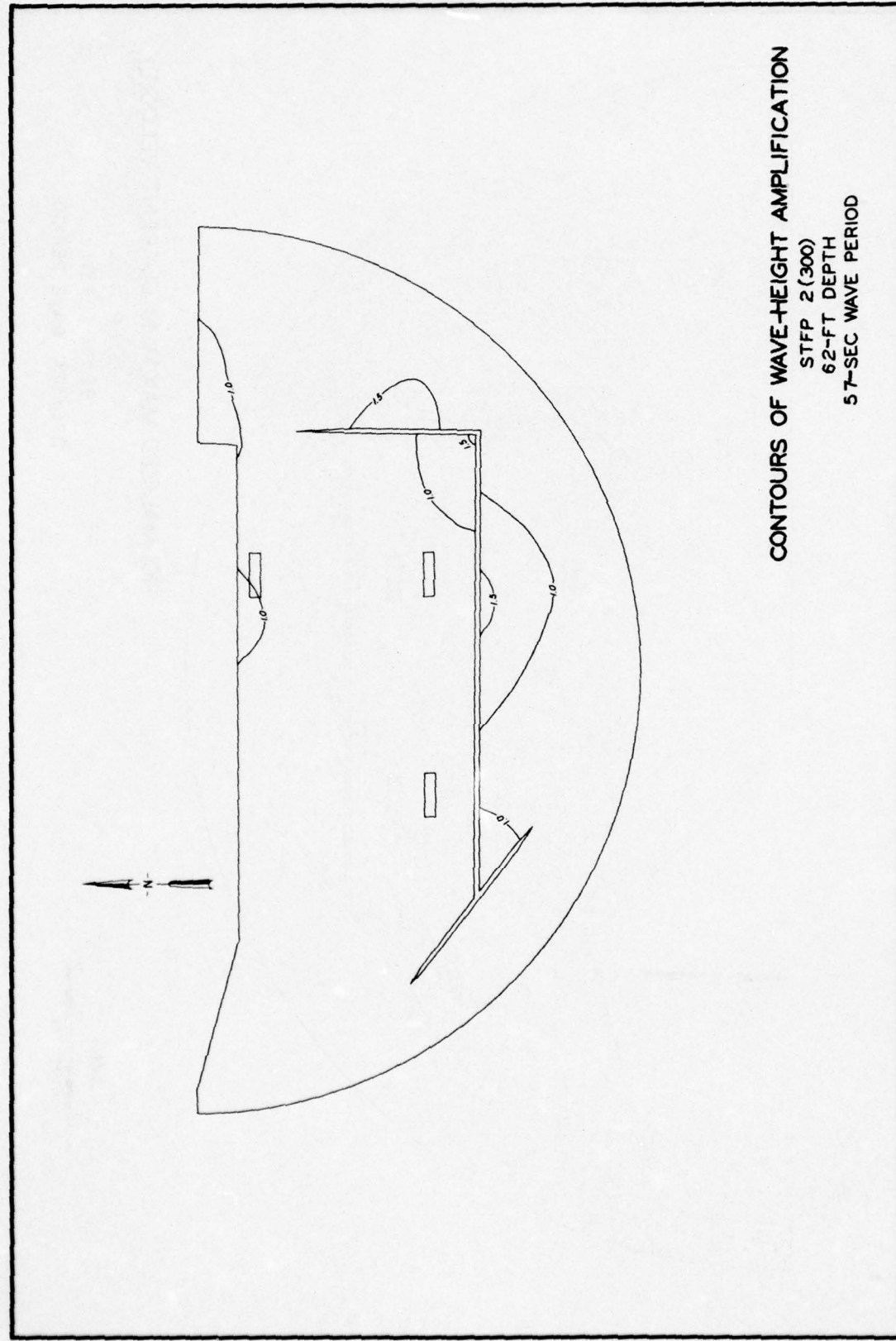
STFP 3

82-FT DEPTH

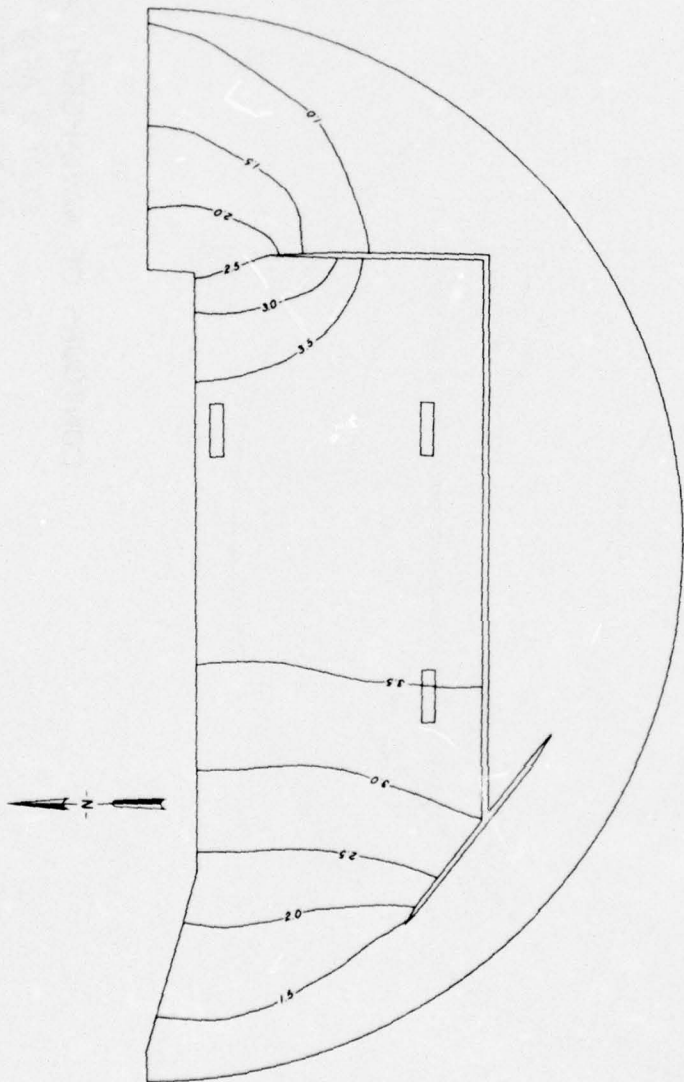
330-SEC WAVE PERIOD



CONTOURS OF WAVE HEIGHT AMPLIFICATION  
STFP 2 (300)  
62-FT DEPTH  
5.7-SEC WAVE PERIOD



CONTOURS OF WAVE-HEIGHT AMPLIFICATION  
STFP 2 (300)  
62-FT DEPTH  
280-SEC WAVE PERIOD

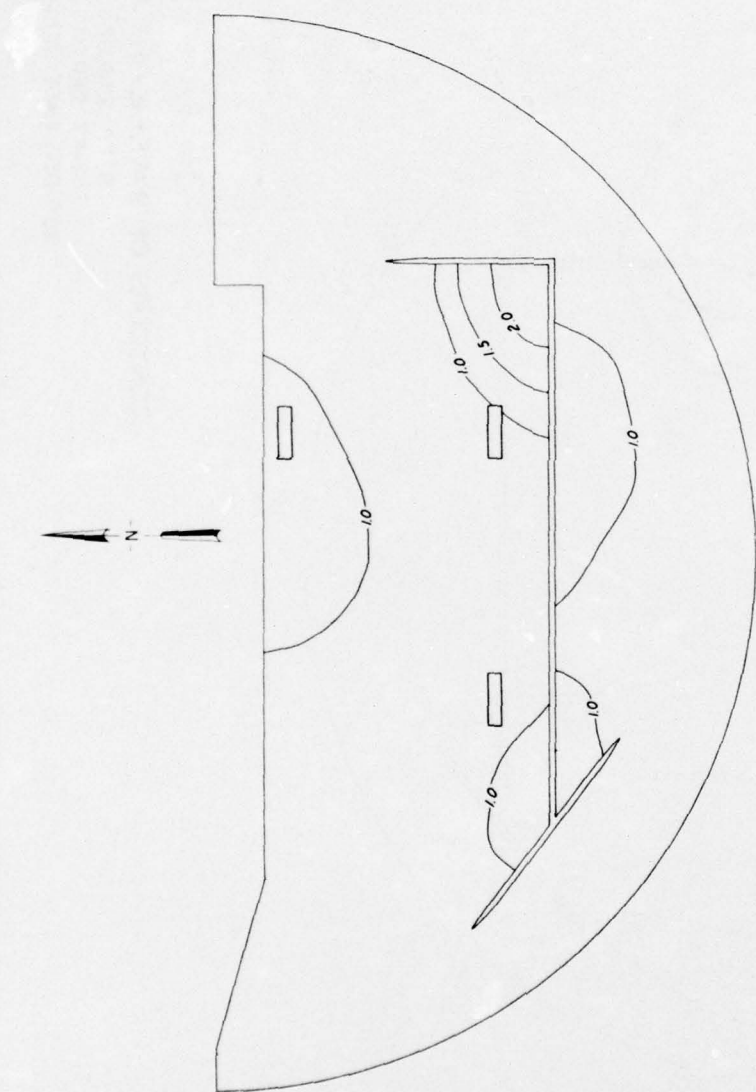


CONTOURS OF WAVE-HEIGHT AMPLIFICATION

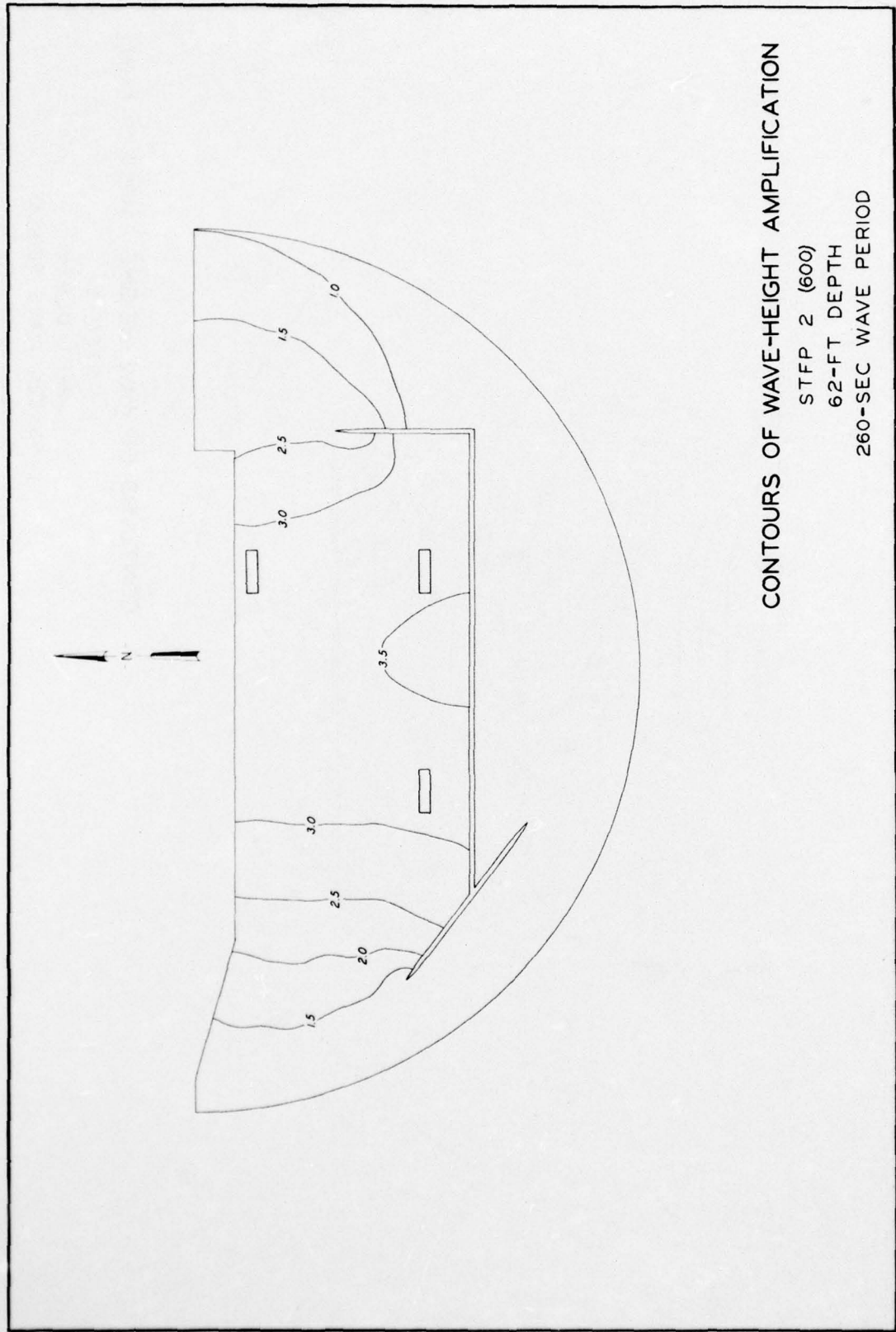
STFP 2 (600)

62-FT DEPTH

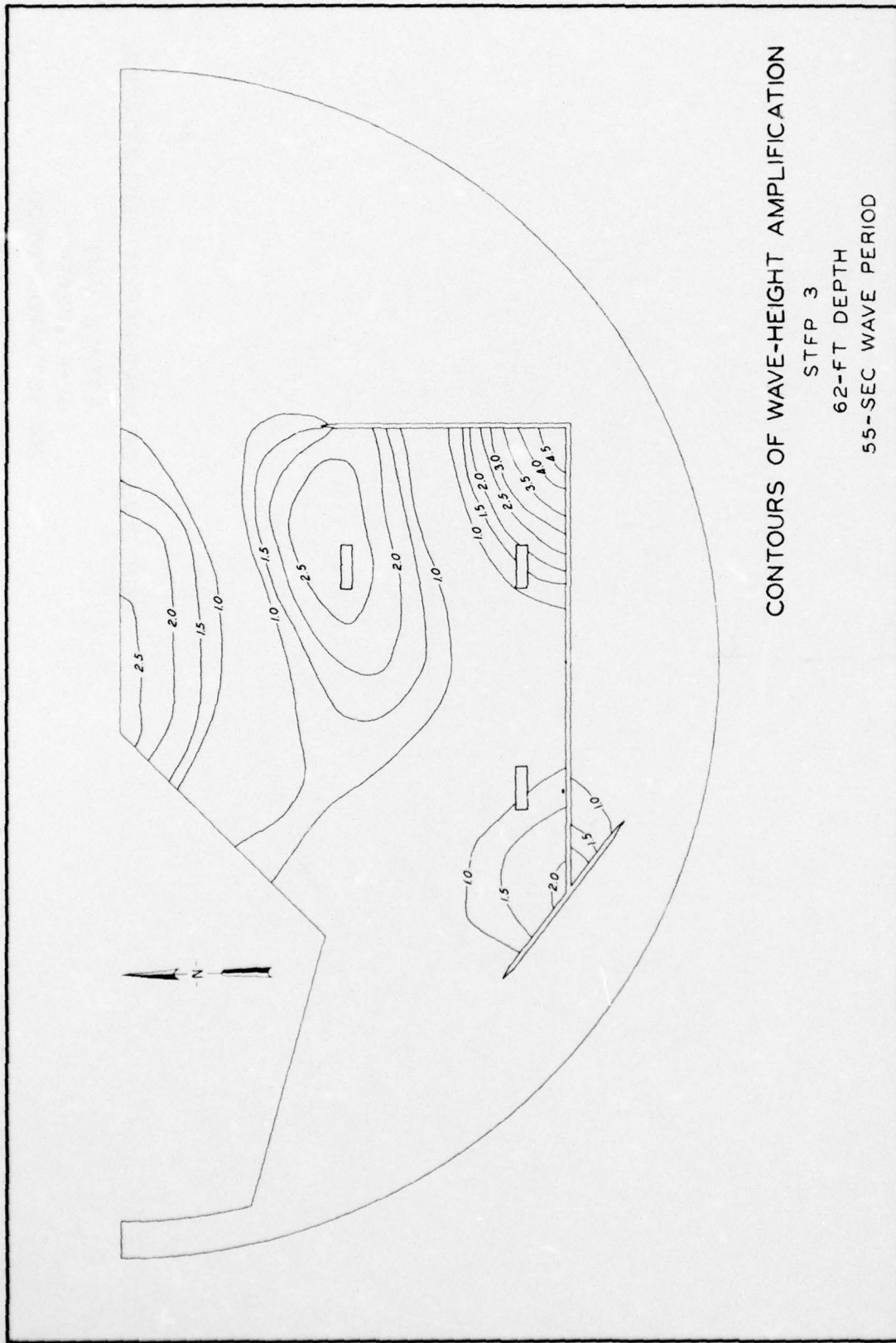
57.5-SEC WAVE PERIOD



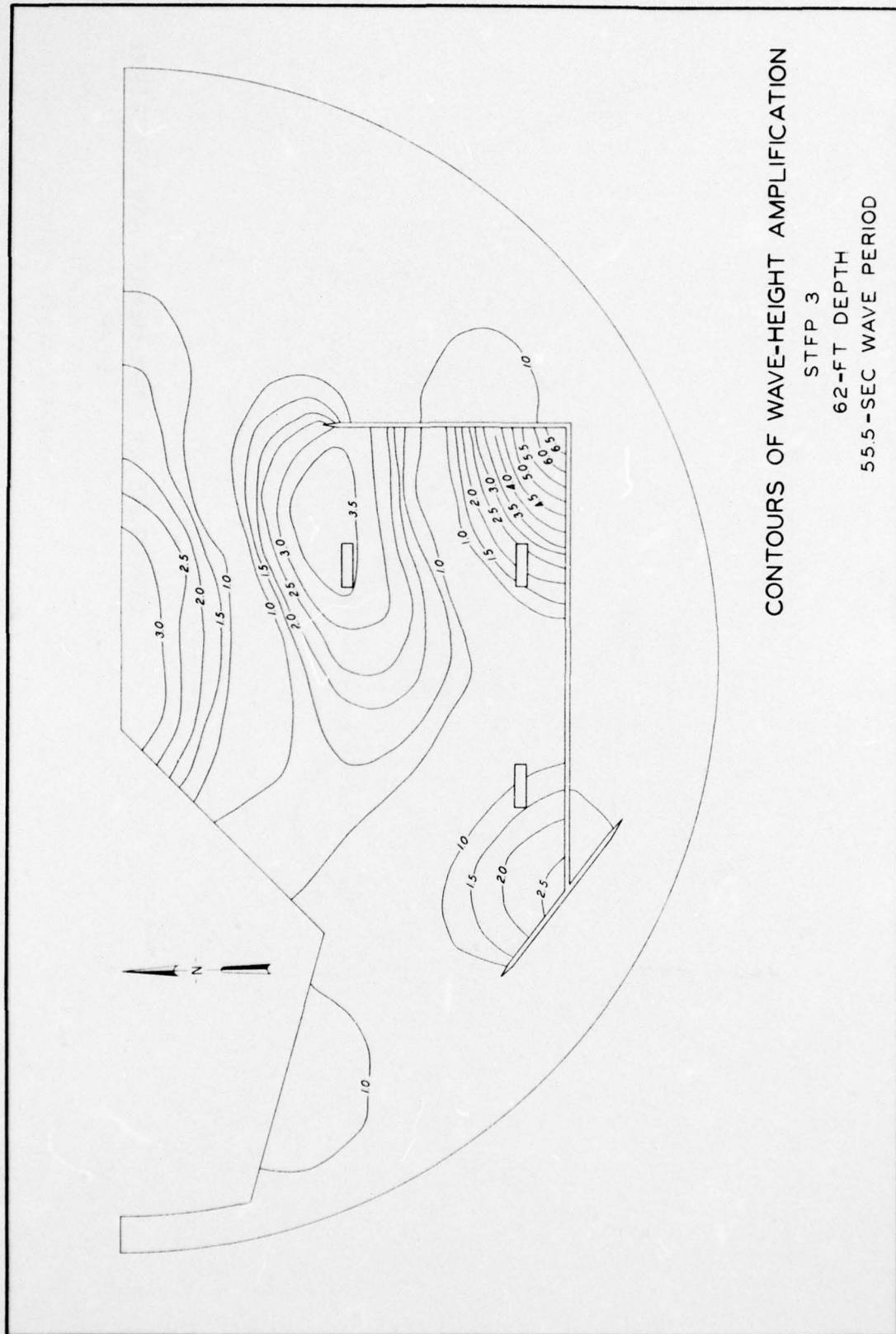
CONTOURS OF WAVE-HEIGHT AMPLIFICATION  
STFP 2 (600)  
62-FT DEPTH  
260-SEC WAVE PERIOD



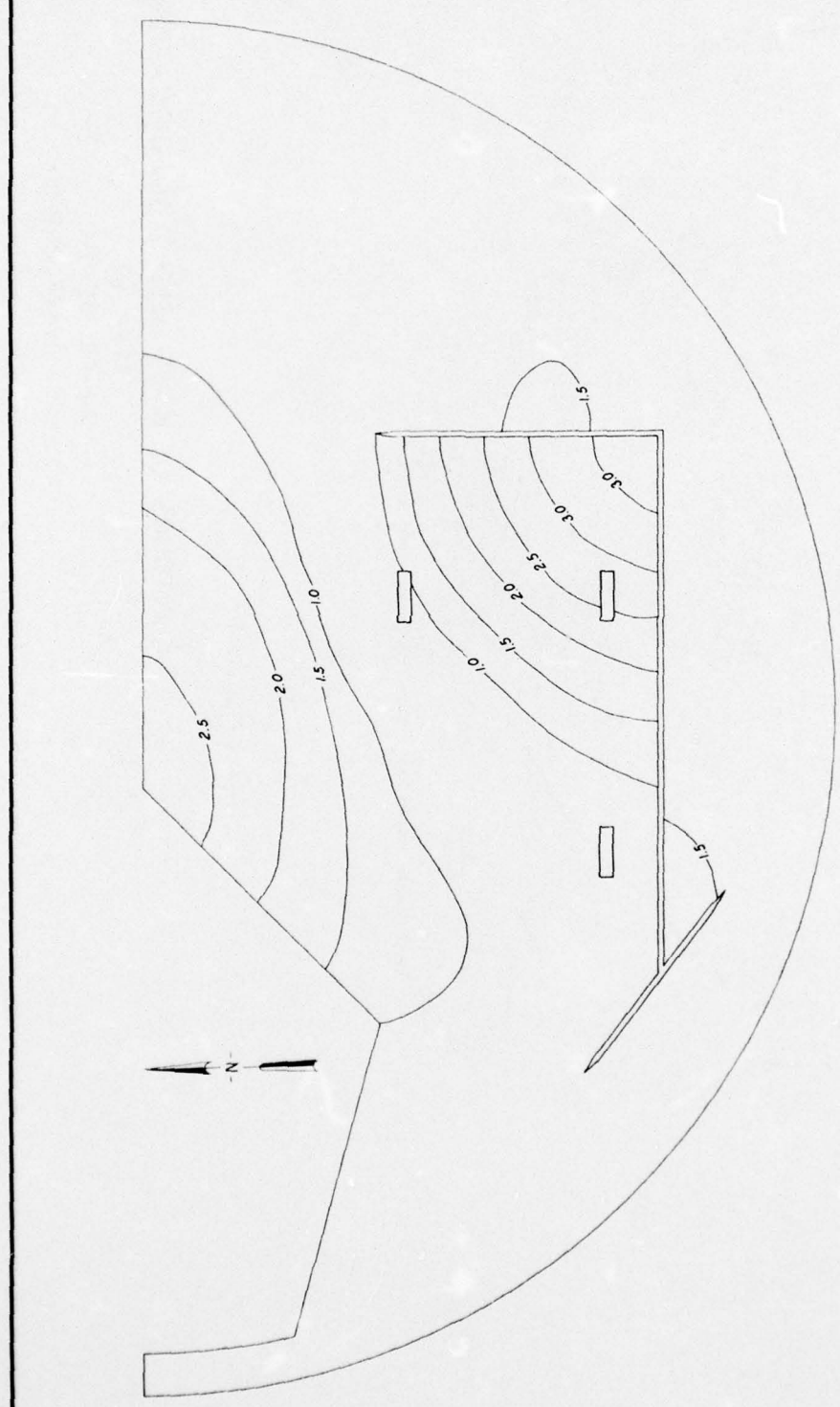
CONTOURS OF WAVE-HEIGHT AMPLIFICATION  
STFP 3  
62-FT DEPTH  
55-SEC WAVE PERIOD



CONTOURS OF WAVE-HEIGHT AMPLIFICATION  
STFP 3  
62-FT DEPTH  
5.5-SEC WAVE PERIOD



CONTOURS OF WAVE-HEIGHT AMPLIFICATION  
STFP 3  
62-FT DEPTH  
106-SEC WAVE PERIOD

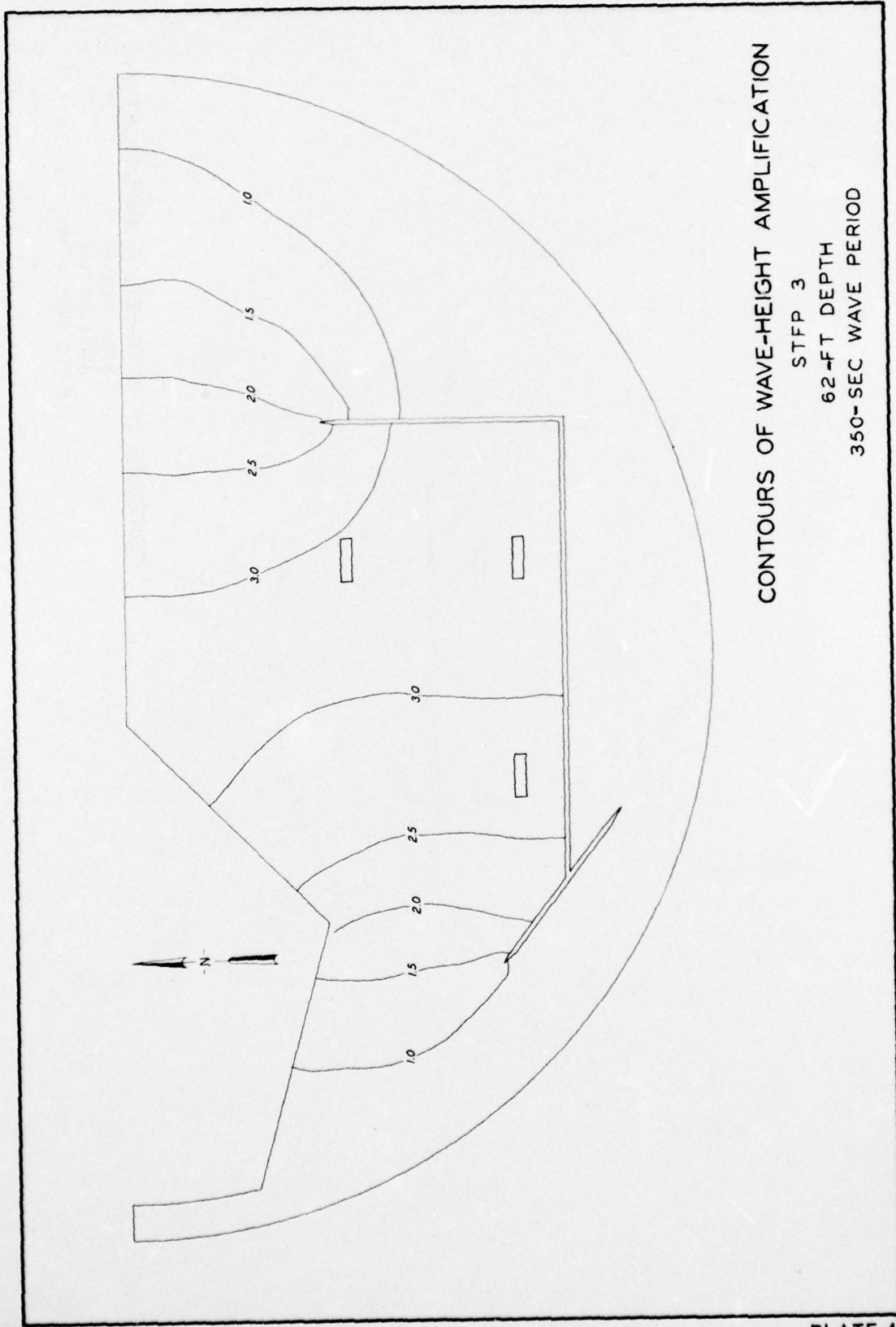


CONTOURS OF WAVE-HEIGHT AMPLIFICATION

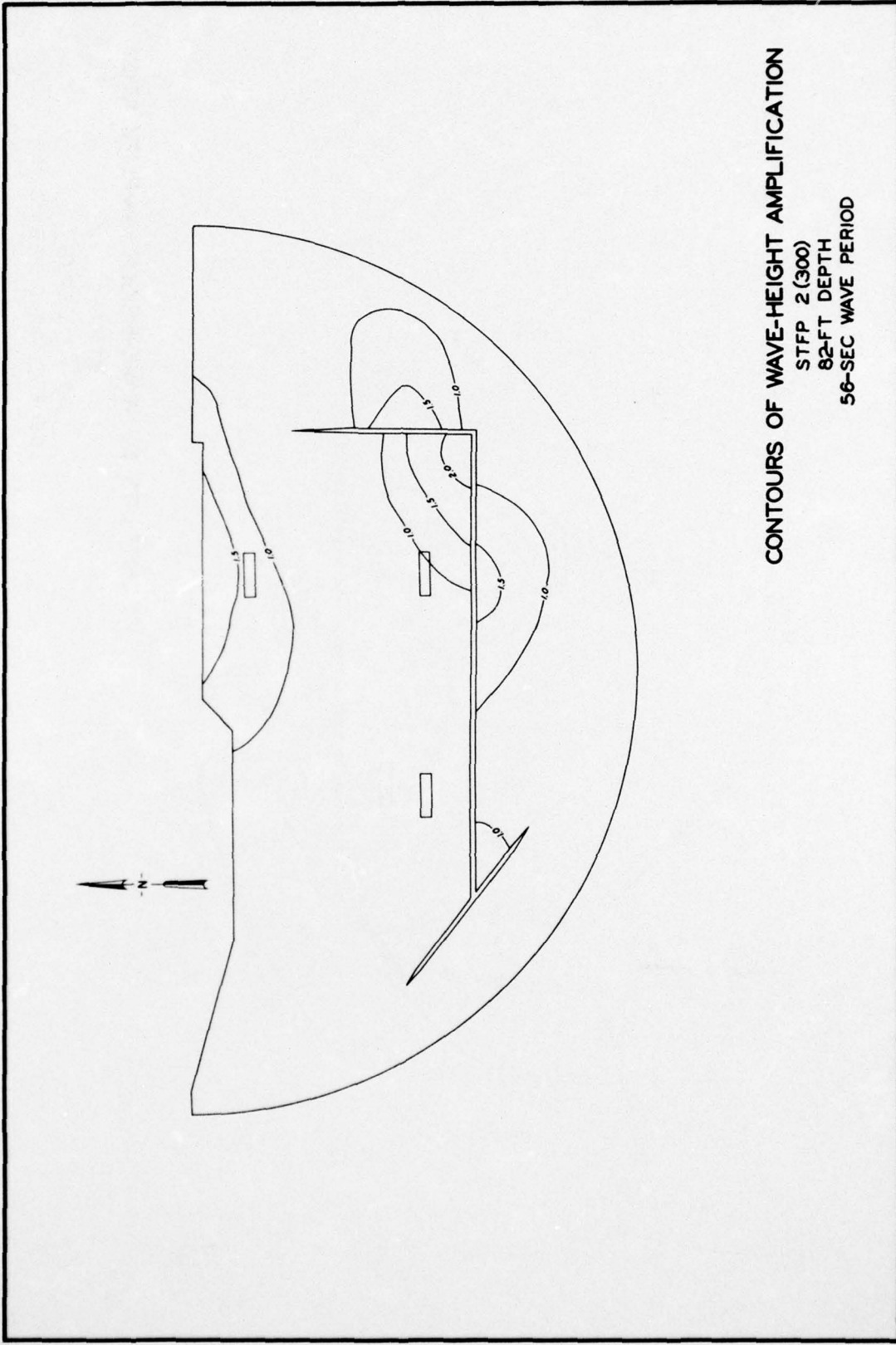
STFP 3

62-FT DEPTH

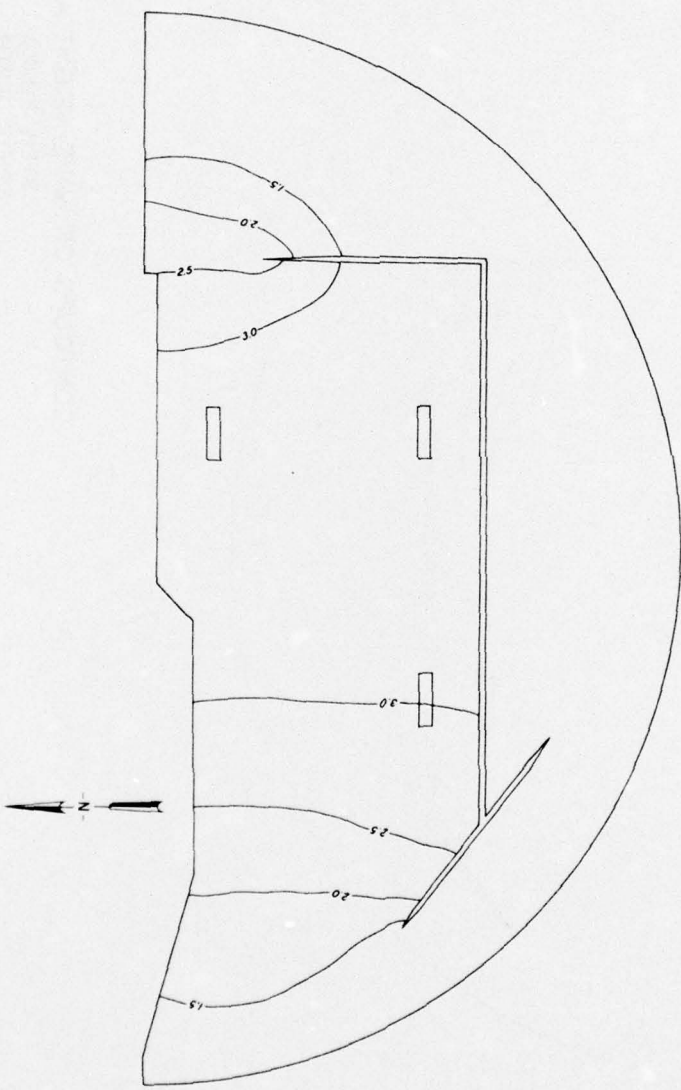
350- SEC WAVE PERIOD



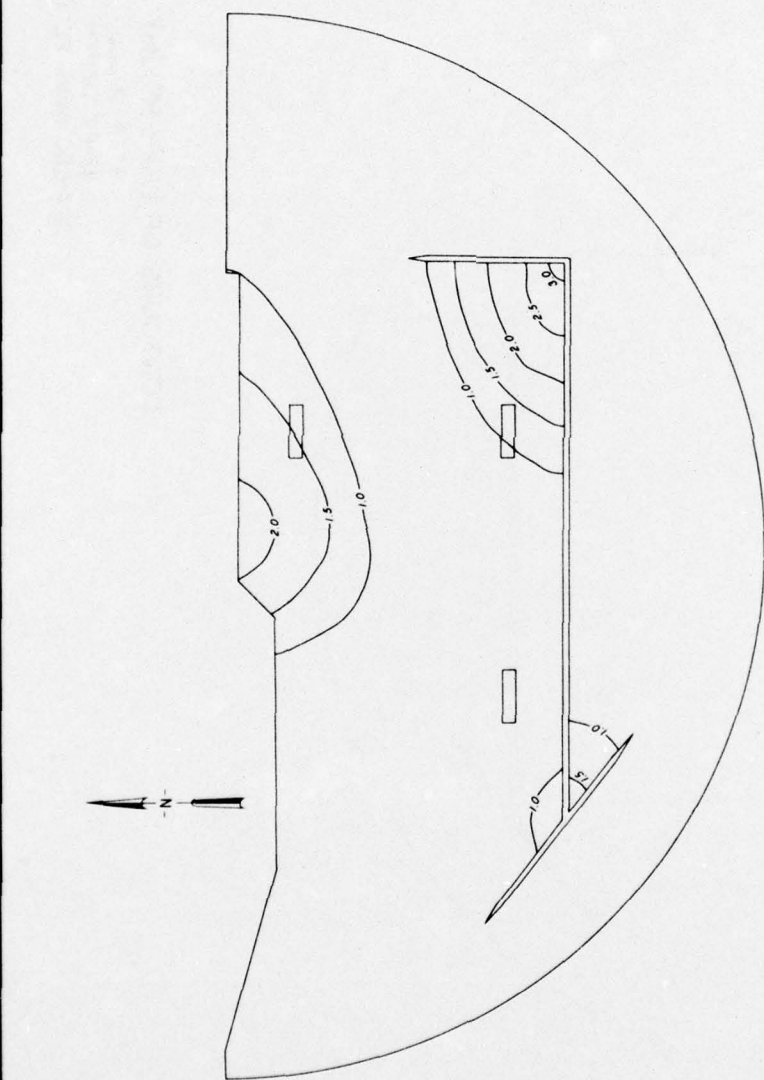
CONTOURS OF WAVE-HEIGHT AMPLIFICATION  
STFP 2 (300)  
82 FT DEPTH  
56 SEC WAVE PERIOD



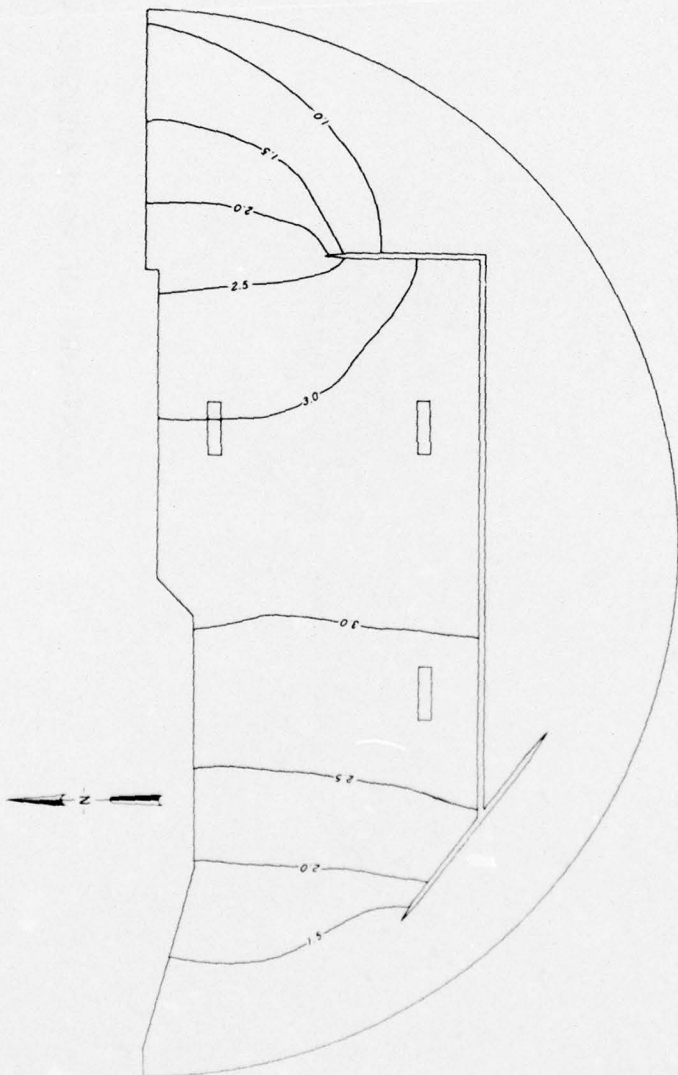
CONTOURS OF WAVE-HEIGHT AMPLIFICATION  
STFP 2 (300)  
82-FT DEPTH  
270-SEC WAVE PERIOD



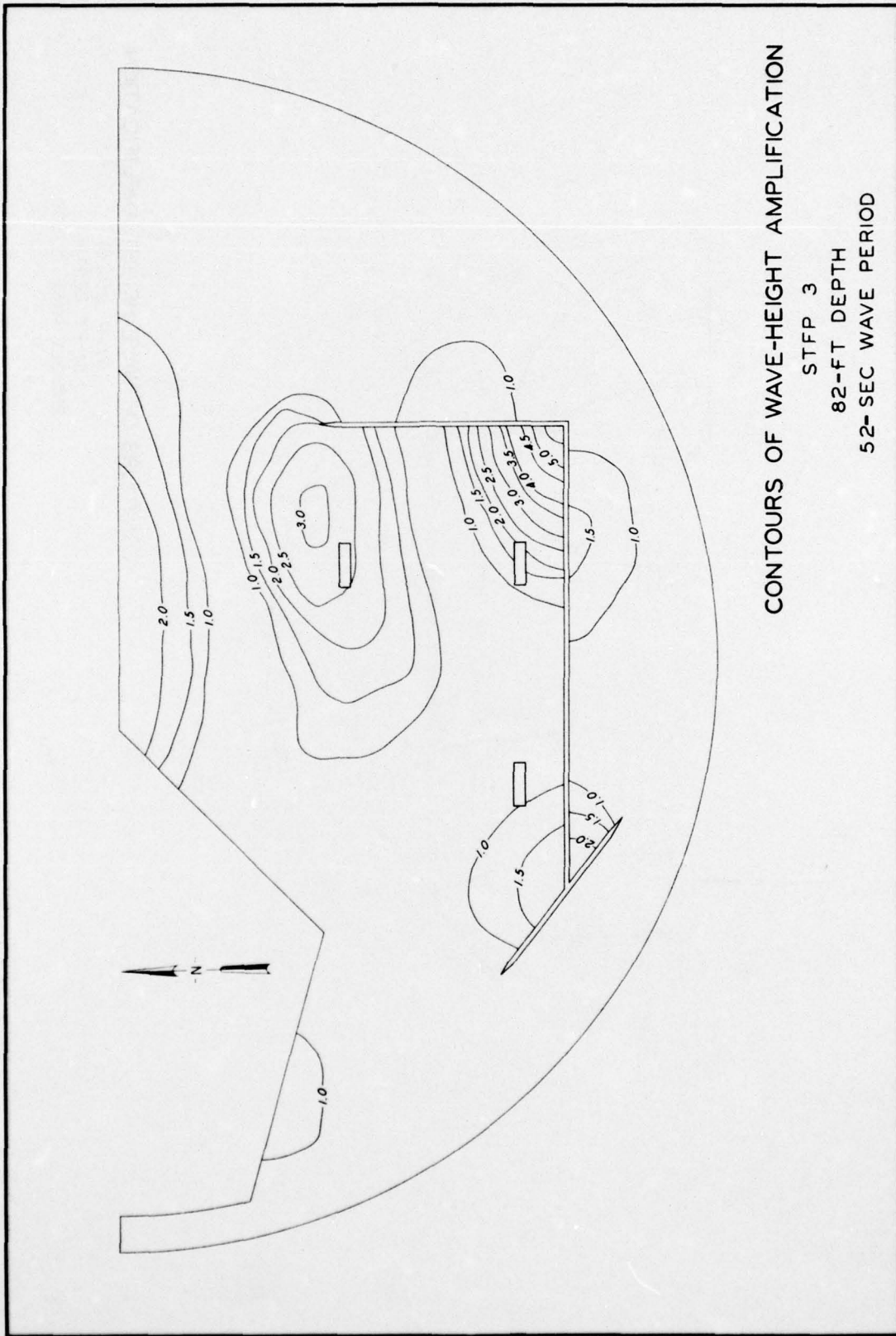
CONTOURS OF WAVE-HEIGHT AMPLIFICATION  
STFP 2 (600)  
82 FT DEPTH  
55.5 SEC WAVE PERIOD



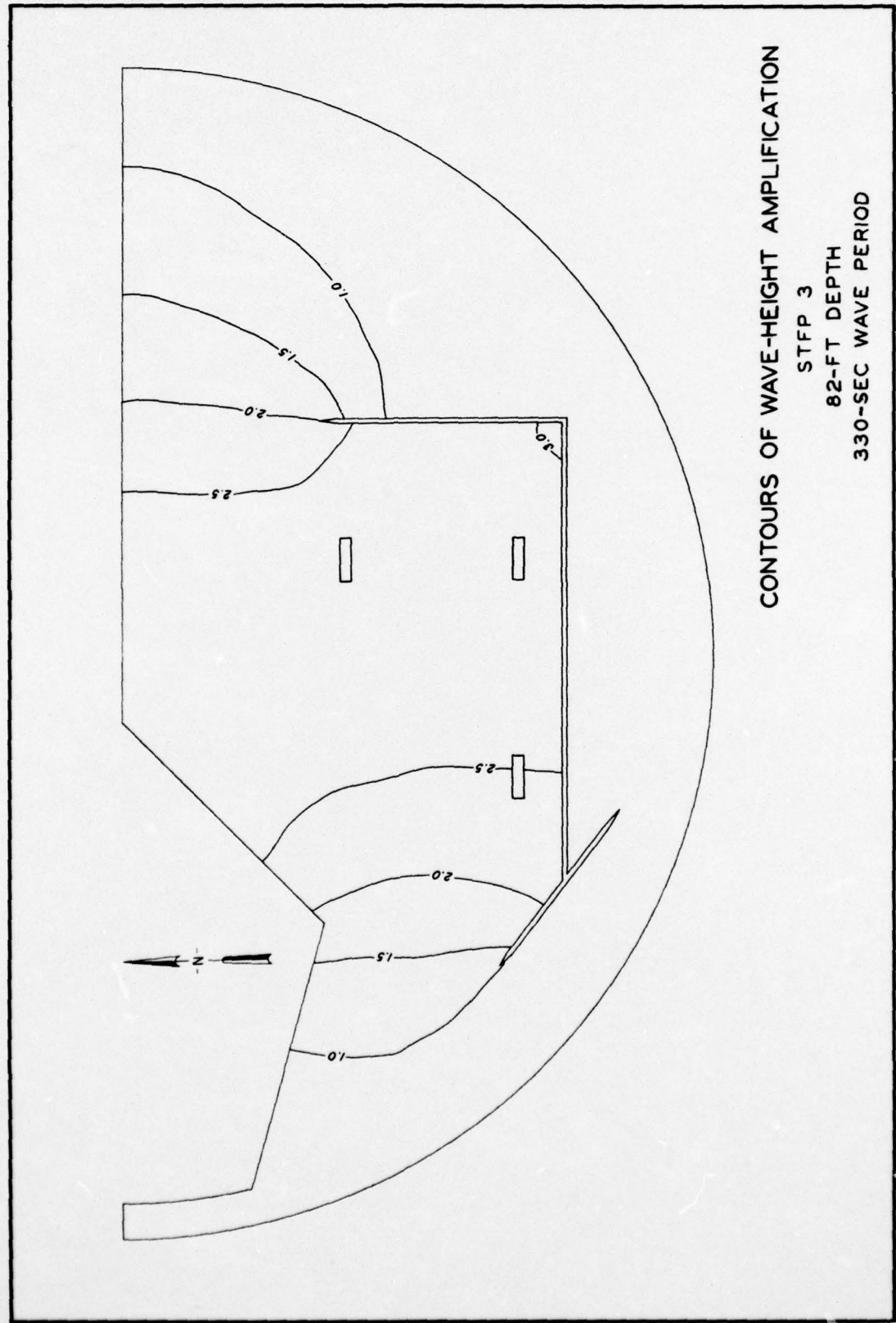
CONTOURS OF WAVE-HEIGHT AMPLIFICATION  
STFP 2(600)  
82 FT DEPTH  
255 SEC WAVE PERIOD



CONTOURS OF WAVE-HEIGHT AMPLIFICATION  
STFP 3  
82-FT DEPTH  
52- SEC WAVE PERIOD



CONTOURS OF WAVE-HEIGHT AMPLIFICATION  
STFP 3  
82-FT DEPTH  
330-SEC WAVE PERIOD



## APPENDIX A: NOTATION

a	Boundary of region A
A	Area of region inside a harbor
g	Acceleration due to gravity, $32.2 \text{ ft/sec}^2$
h	Water depth, ft
$H_n$	Hankel function of the first kind of order n
i	Imaginary number
k	Wave number, $\text{ft}^{-1}$
n	Integer
$n_a$	Unit vector normal to boundary a
r	Spherical coordinate, ft
t	Time, sec
u	Velocity in x-direction, ft/sec
v	Velocity in y-direction, ft/sec
w	Angular velocity, radians/sec
x	Cartesian coordinate, ft
y	Cartesian coordinate, ft
$\alpha_n$	Unknown coefficient
$\nabla$	Gradient, $\text{ft}^{-1}$
n	Wave amplitude, ft
$\phi$	Total velocity potential, $\text{ft}^2/\text{sec}$
$\theta$	Spherical coordinate, degrees
$\phi_a$	Total velocity potential evaluated on boundary a, $\text{ft}^2/\text{sec}$
$\phi_I$	Incident velocity potential, $\text{ft}^2/\text{sec}$
$\phi_R$	Far field velocity potential, $\text{ft}^2/\text{sec}$
$\phi_s$	Scattered velocity potential, $\text{ft}^2/\text{sec}$

In accordance with ER 70-2-3, paragraph 6c(1)(b),  
dated 15 February 1973, a facsimile catalog card  
in Library of Congress format is reproduced below.

Houston, James R

Long Beach Harbor numerical analysis of harbor  
oscillations; Report 3: Alternate plans for Pier J  
completion and tanker terminal project (62- and 82-  
ft depths), by James R. Houston. Vicksburg, U. S.  
Army Engineer Waterways Experiment Station, 1976.

1 v. (various pagings) illus. 27 cm. (U. S.  
Waterways Experiment Station. Miscellaneous paper  
H-76-20, Report 3)

Prepared for Port of Long Beach, Long Beach California.

1. Finite element method.
  2. Harbor oscillations.
  3. Long Beach Harbor.
  4. Mathematical models.
  5. Numerical analysis.
  6. Piers (Docks).
  7. Tanker terminals.
- I. Port of Long Beach. (Series: U. S.  
Waterways Experiment Station, Vicksburg, Miss. Mis-  
cellaneous paper H-76-20, Report 3)  
TA7.W34m no.H-76-20 Report 3